Insulin Estimation and Prediction

A review on the estimation and prediction of subcutaneous insulin pharmacokinetics in closed-loop glucose control

Jorge Bondia, Sergio Romero-Vivó,
Beatriz Ricarte, and José Luis Díez
POC: J. Bondia (jbondia@isa.upv.es)
January 27, 2017

Patients affected by type 1 diabetes suffer from lack of insulin secretion by the pancreas due to the autoimmune destruction of the insulin-producing beta cells. This translates into elevated plasma glucose concentration with deleterious effects in the cardiovascular system that leads to serious long-term complications. With the improvement of continuous glucose monitoring technology, a significant amount of research has been focused in the last decade on the development of an artificial pancreas, that is, a closed-loop glucose control system that automatically dispenses insulin. The artificial pancreas is nowadays closer to reality [1]. Indeed, an artificial pancreas system was approved for the first time by the Food and Drug Administration (FDA) in United States in September 2016 [2], although the system still needs user intervention at mealtime, as currently done in open-loop insulin pump therapy, to administer an insulin bolus based on carbohydrate counting (it is a "hybrid" closed-loop system). A first-generation artificial pancreas is thus expected to be commercially available soon. However, there still remain issues to be addressed for the performance improvement of the artificial pancreas, such as inter- and intra-subject physiological variability, efficient compensation of real-life disturbances (exercise, alcohol, diseases, etc.), pump faults, sensor accuracy and large dynamic lags induced by the subcutaneous administration of insulin. This last challenge constitutes the focus of this article.

Insulin is a glucose-lowering hormone that promotes glucose transport through the cell membrane for its consumption or storage. Glucose regulation is completed in the human body through counterregulatory hormones, such as glucagon that promotes glucose production by the liver resulting in an increase of blood glucose concentration. However, glucagon secretion by the alpha cells in the pancreas is also affected as the disease progresses along time, increasing the risk of suffering hypoglycemia. Severe hypoglycemia can provoke comma and death.

Unidirectional effect of insulin has major implications in the design of an artificial pancreas. This is aggravated by the significant lag introduced by subcutaneous insulin infusion, which

is currently the safest infusion route for a commercial artificial pancreas, as opposed to the endogenous pancreas that secretes insulin directly into portal circulation (the vessels that connect the pancreas and other organs with the liver, which acts as a first blood filter before entering the main circulatory system). Even in approaches with concomitant infusion of glucagon (the so-called dual-hormone artificial pancreas), mechanisms are necessary to avoid an excess of insulin delivery which may lead to late hypoglycemia putting at stake the patient's safety. Independently of how these mechanisms are incorporated into the control schemes, all of them must rely on pharmacokinetic models predicting either circulating plasma insulin or a measure of "insulin-on-board", such as the insulin depot remaining at the subcutaneous tissue before entering circulation. In this article, methods to constrain insulin delivery are reviewed, as well as the subcutaneous insulin pharmacokinetic models and estimators on which they rely upon.

A big challenge in the prediction of physiological signals, such as insulin concentration, is the large intra-subject variability that patients suffer. Indeed, in terms of control engineering, a patient is a highly time-varying uncertain plant. The intra-day and day-to-day patient's behavior change due to circadian rhythms (24-hour rhythmic physiological oscillations driven by the body clock, for instance, daily patterns in insulin sensitivity), and other multiple sources of uncertainty arise in key physiological processes such as meal absorption and subcutaneous insulin absorption. Despite this fact, the use of population models for the prediction of insulin pharmacokinetics, that is, how the infused insulin appears in blood, is still common practice.

The impact of variability on the model prediction and its implication in closed-loop performance is analyzed. Nevertheless, large intra-subject variability suggests that real-time state and pharmacokinetic parameters estimation is convenient, even when individualized models are considered. The availability of continuous glucose measurements allows to address this problem should an observable glucose-insulin model be available. Different observer techniques proposed to this purpose are reviewed and discussed.

The subcutaneous insulin route

The pancreas secretes insulin into the portal vein towards the liver, which acts as a first filter before insulin reaches systemic circulation. In the liver, insulin promotes glucose storage in hepatic cells decreasing glucose production. In the fat and muscle cells, insulin acts as a key that triggers the mobilization of glucose transporters to the cell membrane promoting glucose uptake by the cell. As a result of both actions, plasma glucose concentration decreases. The dynamic lag of insulin action is estimated to be about 30 minutes [3].

An artificial pancreas is a classic closed-loop glucose control system (see Figure 1) that

automatically dispenses insulin to a patient (the process), and has three main components: the continuous glucose monitor (the sensor), the insulin infusion pump (the actuator) and the control algorithm (the controller). Contrary to the pancreas, an artificial pancreas cannot have direct access to the hepatic portal circulation for insulin infusion. Implantable insulin pumps that infuse insulin into the peritoneum, that is, the body cavity containing the abdominal organs, were proposed [4] in an attempt to emulate as close as possible the pancreas. However, nowadays, external insulin pumps that infuse insulin through the skin (the so-called subcutaneous route) are the only ones considered feasible for a commercial artificial pancreas due to their minimal invasiveness. External insulin pumps were first introduced in the 1980s and they are nowadays a well-established open-loop insulin therapy [5]. Traditional pumps infuse insulin through a small, flexible tube (a catheter) with a needle allocated into the fat layer under the dermis (the subcutaneous adipose tissue). Patch pumps with no visible catheter are also available [6].

Insulin pumps make use of fast-acting insulin analogs, like insulin aspart [7] or insulin lispro [8], which are synthetic insulin molecules with some modification in the amino acid chain compared to human insulin in order to speed up subcutaneous absorption and get a faster insulin action. No significant differences in pharmacokinetics and metabolic effects between insulin aspart and lispro are found [9]. Insulin molecules can be in the form of hexamers (groups of six molecules), dimers (groups of two molecules) or monomers (a single molecule). Once infused at the subcutaneous tissue, the generated insulin depot starts diffusing from the infusion site while dissociation of hexamers into dimers and monomers happen. Insulin analogs molecule structure is designed to facilitate this dissociation, since only dimers and monomers are small enough to go through the capillary wall and thus be absorbed towards circulation [10]. The lag introduced by subcutaneous absorption is estimated to be about 50 minutes [3].

Subcutaneous insulin pumps are combined with subcutaneous needle-type continuous glucose monitors that compute plasma glucose values from electrochemical measurements of interstitial glucose. Dynamics of glucose transport between plasma and the interstitial fluid introduce a measurement lag estimated in about 10 minutes [3].

Thus, the lag induced by the subcutaneous route adds up to 90 minutes since insulin is infused until its peak effect (50 minutes for insulin absorption, 30 minutes for insulin action, and 10 minutes for glucose measurement). This significant dynamic lag poses an important challenge to glucose control, especially because once insulin is infused, its effect cannot be easily counteracted by the controller, unless the patient eats carbohydrates as rescue. Only dual-hormone artificial pancreas systems can counteract an insulin excess with glucagon infusion at the expense of much higher system complexity. However, glucagon administration must also be limited since its excess may produce side effects such as nausea and vomiting [11]. Thus,

mechanisms are necessary to avoid an excess of insulin delivery due to controller's over-actuation, since it may lead to late hypoglycemia putting at stake the patient's safety. These mechanisms constitute a critical component of any artificial pancreas.

Large intra-subject physiological variability is an additional important challenge for the artificial pancreas and it is responsible, at least in part, for the difficulties of achieving a good glycemic control. Nowadays, patients still have an average exposure to hypoglycemia (< 70 mg/dL) over 1 h/day and to hyperglycemia (> 180 mg/dL) higher than 9 h/day [12]. The sources of physiological variability are not fully understood although variability of subcutaneous insulin absorption [13], [14] and changes of insulin sensitivity (due to circadian rhythms [15] and premenstrual periods in women [16]) seem to play a major role. Meal ingestion also has a highly variable effect on glucose homeostasis [17].

Indeed, an intra-subject variability of 27% was reported for time-to-peak plasma insulin concentration (parameter t_{maxI} in model (26)-(28)) in a pharmacokinetic study of insulin aspart in subjects with type 1 diabetes [13]. Nearly 40% of this variability was attributed to variations in depth of cannula insertion, insulin site age and local tissue perfusion. In contrast, insulin clearance was highly reproducible in the same study. A recent study with insulin lispro also showed an important impact of lypohypertrophia (the accumulation of abnormal mass of fat under the skin) of the insulin injection site on insulin absorption and insulin effect [18]. Lypohypertrophia appears when the same injection site is used repeatedly and it is characterized by hypertrophic adipocytes, reduced vascularization and lower capillary density. Although patients are advised to rotate the injection site, a prevalence of lypohypertrophia ranging from 28% to over 64% is reported, depending on the country, being more frequent in type 1 diabetes [18]. Compared to normal adipose tissue, lypohypertrophia increased substantially intra-subject variability both in pharmacokinetic and pharmacodynamic parameters. The coefficient of variance (CV) of the area-under-the-curve of plasma insulin after an insulin injection in lypohypertrophic adipose tissue ranged from 55% to 65% (compared to 11% to 20% for normal adipose tissue), corresponding to a 3- to 5-fold increment. No effect of lypohypertrophia on the time-to-peak plasma insulin was found. Intra-subject variability of insulin effect (measured as the area-under-the-curve of the exogenous glucose infusion needed to keep plasma glucose constant after insulin injection) was generally higher, especially during the first hour when CV reached 90% (compared to 66% for normal adipose tissue).

Although the above study was carried out with insulin injections and not an insulin pump, it highlights the challenge that intra-subject variability poses for any insulin therapy with subcutaneous administration, including an artificial pancreas. Current insulin infusion sets in pumps need to be replaced every 2 to 3 days to avoid inflammation and infection. Differences

in insulin absorption of consecutive infusion sites due to the development of lypohypertrophia can jeopardize the artificial pancreas performance, increasing the risk of hypoglycemia. Besides, current systems need two skin punctures, one for the sensor and one for the insulin pump, making more difficult the rotation of the infusion site [19].

Glucose-insulin models

Models describing the glucose regulation by insulin (henceforth referred as glucose-insulin models) are needed for controllers and observers design. The reader is referred to the reviews in [20] and [21] for a historical perspective on modeling the glucose-insulin system, including models to measure key physiological signals or parameters in glucose metabolism (the so-called minimal models), fine-grained models aiming at a detailed description of the physiological processes for simulation purposes (maximal models) and models for control with a simpler structure capturing the most relevant dynamics.

Independently of the model complexity, the description of glucose metabolism in the context of any subcutaneous insulin therapy such as the artificial pancreas implies the following model components (see Figure 2):

1) A subcutaneous insulin pharmacokinetic model describing how insulin appears in blood after subcutaneous infusion. Although modeling of subcutaneous insulin pharmacokinetics dates back to the 80s, only works related to the fast-insulin analogues currently used in insulin pump therapy are relevant here (insulin lispro and aspart), as well as new insulin formulations under investigation for ultra-fast insulin absorption, for instance.
2) An insulin action model describing how plasma insulin concentration exerts its effect on glucose metabolism. This component involves mainly the transport lags from plasma to the insulin action site.
3) A carbohydrate digestion and absorption model describing how glucose enters blood after a meal. This model has proven to be challenging due to the complex physiology of gastric emptying and intestinal absorption and the lack of glucose absorption rate measurements unless complex clinical studies are conducted.
4) A glucose metabolism model describing the comprehensive effect of insulin and meals on plasma glucose concentration. More complex models may also include other effects like glucagon and exercise.

Three widely used models in the artificial pancreas community, from lower to higher complexity, are Bergman model (minimal) [22], Hovorka model (intermediate complexity) [23] and Dalla Man model (maximal) [24]. This latter is the core of the UVA-PADOVA type 1

diabetes simulator [25], a simulation tool for the evaluation of glucose controllers accepted by the FDA as a substitute of animal trials. Since models for simulation are not in the scope of this article, it will not be presented here for the sake of simplicity.

Table 1 presents the equations for the Bergman and Hovorka models (left and center columns). Bergman model originated in 1979 [26] to describe the intravenous glucose tolerance test (IVGTT), a clinical test to analyze how the body metabolizes glucose. It consists in the infusion of glucose intravenously and the measurement of plasma glucose and insulin concentrations for a certain time before and after the infusion. From these measurements, an index of insulin action, the so-called insulin sensitivity, is computed by means of a parsimonious (minimal) model. Bergman model is a second order non-linear model relating plasma insulin concentration $I(t)$ (input) and plasma glucose concentration $G(t)$ (output). Insulin effect, $X(t)$, is modeled with a first-order system representing a lagged action of insulin. Plasma glucose concentration, $G(t)$, is inhibited by glucose itself and insulin effect. A constant hepatic glucose production $p_1 G_b$ is considered that drives the system to equilibrium for a basal insulin concentration I_b. Finally, the term $U_G(t)/V_G$ describes the intravenous glucose infusion (or glucose rate of appearance from the meal when a meal model is interconnected). Parameters p_1, p_2 and p_3 are kinetic parameters. Parameter p_1 is called "glucose effectiveness" and it represents glucose auto-inhibition. Insulin sensitivity is computed as p_3/p_2. Bergman model was conceived as a model for measuring. This is the reason why no subcutaneous insulin absorption or meal ingestion is considered.

Hovorka model [23], [27] (see Table 1) is a 7-th order non-linear model that includes all model components in Figure 2. Carbohydrate digestion and absorption is described by the impulse response of a second order linear model, with input D_G the amount of carbohydrate in the meal, and output the glucose rate of appearance in blood, $U_G(t)$. Parameter A_G is the carbohydrate bioavailability, that is, the fraction of carbohydrate in the meal that will finally reach blood, and t_{maxG} is the time constant. Subcutaneous insulin pharmacokinetics is a 3-rd linear model. Subcutaneous absorption shares the same model structure as the meal model, with $u(t)$ the insulin infusion from the pump and states $S_1(t)$ and $S_2(t)$ representing mass of insulin along subcutaneous tissue, with transport time constant t_{maxI}. Insulin rate of appearance in blood is $S_2(t)/t_{maxI}$, that, once converted to concentration rate by dividing by the insulin distribution volume V_I, enters the first-order kinetic equation defining plasma insulin concentration, $I(t)$. Parameter k_e is the fractional elimination rate. Plasma insulin exerts three actions, following a first-order dynamics (representing a "remote" action): $X_1(t)$ is the effect of insulin on glucose distribution/transport, $X_2(t)$ the effect on glucose disposal (it promotes glucose entering muscle and adipose tissue cells) and $X_3(t)$ the effect endogenous glucose production (it inhibits glucose

production by the liver). Constants k_{ai}, $i = 1, 2, 3$, are kinetic constants and k_{bi}/k_{ai} are the insulin sensitivities for each effect. Finally, states $Q_1(t)$ and $Q_2(t)$ represent the glucose mass in plasma and interstitial tissue, respectively. Transport of glucose between both compartments happens at rates k_{12} and $X_1(t)$, depending on the direction. Besides these transport flows, glucose from the meal, $U_G(t)$, and hepatic glucose production $EGP_0(1 - X_3(t))$, with EGP_0 the production extrapolated to zero insulin, are input flows to the plasma compartment; insulin-independent consumption (mainly by brain), $F_{01}^c(t)$, and renal glucose elimination, $F_R(t)$ are output flows. For the sake of simplicity, the reader is referred to [23] for the definition of $F_{01}^c(t)$ and $F_R(t)$. Regarding the interstitial compartment, aside the inter-compartment transport, glucose uptake by muscle and adipose tissue, $X_2(t)Q_2(t)$ is an output flow. Plasma glucose concentration (model output) is finally given by $Q_1(t)/V_G$, where V_G is the glucose distribution volume.

Due to its simplicity and identifiability properties, Bergman model is widely used outside its original scope, in combination with a subcutaneous insulin pharmacokinetic and a carbohydrate absorption model. An example is the so-called "Identifiable Virtual Patient" model [28], also presented in Table 1 (right column). Carbohydrate absorption is described as in Hovorka model, although the output is divided by the glucose distribution volume V_G for $R_A(t)$ to represent a concentration rate, instead of a mass rate ($R_A(t) = U_G(t)/V_G$). Insulin action and glucose metabolism are equivalent to the Bergman model, with the difference that plasma insulin $I(t)$ is considered, instead of its deviation with respect to basal insulin I_b. State $I_E(t)$ and parameter $GEZI$ (Glucose Effectiveness extrapolated to Zero Insulin) are thus equivalent to $X(t)$ and p_1, respectively, with the change in its meaning due the above difference. Parameter EGP is equivalent to $p_1 G_b$ and describes the hepatic glucose production. The subcutaneous insulin pharmacokinetic model is of relevance here. It consists in a second order linear model with time constants τ_1 and τ_2. Parameter K_{cl} is insulin clearance, that is, how much volume of plasma is cleared of insulin per unit time. Applying Laplace transform, the corresponding transfer function is

$$\frac{I(s)}{u_{SC}(s)} = \frac{\frac{1}{\tau_1}\frac{1}{\tau_2}}{K_{cl}(s + \frac{1}{\tau_1})(s + \frac{1}{\tau_2})}. \tag{1}$$

Its impulse response for an insulin bolus $u_{SC}(t) = U_0\delta(t)$ is

$$I(t) = U_0 \frac{1}{K_{cl}(\tau_2 - \tau_1)} \left(e^{-t/\tau_2} - e^{-t/\tau_1}\right). \tag{2}$$

This is why this model is referred often as "bi-exponential model" [29], [30]. An alternative

state-space representation of model (1) is the compartmental model

$$\frac{dq_1(t)}{dt} = u_{SC}(t) - \frac{1}{\tau_1}q_1(t), \quad (3)$$

$$\frac{dq_2(t)}{dt} = \frac{1}{\tau_1}q_1(t) - \frac{1}{\tau_2}q_2(t), \quad (4)$$

$$I(t) = \frac{q_2(t)}{V_I} = \frac{1/\tau_2}{K_{cl}}q_2(t), \quad (5)$$

where $q_1(t)$ is the mass of insulin at the subcutaneous tissue, $q_2(t)$ is the plasma insulin mass, V_I is the insulin volume of distribution, which is the ratio between insulin clearance (K_{cl}) and insulin elimination rate constant ($1/\tau_2$). It becomes apparent from (3)-(5) that the biexponential model corresponds to the Hovorka subcutaneous insulin pharmacokinetic model with the subcutaneous space simplified to a single compartment and the parameter equivalences $\tau_1 = t_{maxI}$ and $1/\tau_2 = k_e$. Figure 3 shows a comparison of the response of both models to an insulin bolus of 1U, considering published nominal parameters.

Insulin observers

Independently of the control algorithm used in an artificial pancreas, either single-hormone (only insulin) or dual-hormone (insulin and glucagon), mechanisms are necessary to avoid an excess of insulin delivery for safety reasons. These mechanisms must rely on subcutaneous insulin pharmacokinetic models, as the ones described in the previous section, for the estimation of either circulating plasma insulin or insulin-on-board (henceforth referred as IOB for short), which represents the injected, but not still used, insulin that will have an effect in the future. Nevertheless, even with the use of individualized models, real-time estimation of those signals is convenient for an effective closed-loop glucose control, since large intra-subject variability can compromise performance (see sidebar "Models and variability" for details). This problem could be addressed with the design of insulin observers, in case an observable glucose-insulin model is available. The reader is referred to the sidebar "Observability of nonlinear systems" for a description of observability tests applicable to glucose-insulin models in Table 1. An observer is a real-time estimator with a feedback mechanism for recursively correcting its estimated state based on the actual outputs measured from the real physical system. Observers can also be used for real-time estimation of model parameters via a state extension. The Luenberger observer and especially different extensions of the Kalman filter to nonlinear systems (see sidebar "Kalman filter extensions to nonlinear systems") are proposed in literature. Basic knowledge on the Luenberger observer and linear Kalman filter is assumed henceforth. Remark that depending on the modeling framework, the term "observer" (deterministic) or "filter" (stochastic) is used. For instance, Luenberger observer is strictly for deterministic systems whereas the Kalman filter

is formulated in a stochastic framework that incorporates models for measurement and system noise and it produces an explicit estimate for the covariance of the system state.

Observers are integrated into some artificial pancreas systems for several purposes. In [31], a Kalman filter is used in a Model Predictive Control-based system to update two model parameters: (i) a glucose flux quantifying model mismatch; and (ii) carbohydrate bioavailability. A stochastic-based approach incorporating competing models differing in the rate of subcutaneous insulin absorption and action, as well as carbohydrate absorption, are used to account for intra-subject variability. In [32], a Luenberger observer is used to estimate the initial state of the prediction model in a zone MPC system [33]. In [34], its performance is compared to a moving horizon state estimator (MHSE), which is based on a constraint optimization problem that calculates the optimal sequence of the process and the measurement noises to minimize a cost function, within a fixed history horizon. It is shown to have a better performance than Luenberger observer in simulation, rejecting a meal disturbance quicker without inducing hypoglycemia.

However, despite the risk for the patient's safety implied by plasma insulin or insulin-on-board estimation errors due to large intra-subject variability, the number of works in literature addressing the design of insulin observers and, most importantly, assessing its performance with clinical data, is scarce.

Hovorka glucose-insulin model [23] and the Extended Kalman Filter (EKF) are used in [35], where real-time estimation of plasma insulin concentration from continuous glucose monitoring (CGM) measurements in subjects with type 1 diabetes is addressed in the context of insulin observers for closed-loop control. The extra equation

$$\dot{IG}(t) = \frac{1}{\tau}\left(G(t) - IG(t)\right), \tag{6}$$

where $IG(t)$ represents interstitial glucose (what the CGM measures) and τ is the time constant for plasma-to-interstitial space glucose transport, is added to the Hovorka model to describe the lagged measurement by the CGM. Process and observation noises are also added. In addition, state observers are designed to estimate uncertain pharmacokinetic parameters, in particular fractional elimination rate, k_e, and time-to-maximum insulin absorption, t_{maxI} (see Table 1), by building new extended models in which these parameters are considered as new states with no dynamics. The observability of these models is demonstrated analytically through Lie derivatives.

Plasma insulin estimations are validated in both a simulation study, with a total of five meals and 25-hour duration, and a clinical validation, using real data from 12 patients with type 1 diabetes who underwent four mixed meal studies during 5 hours, after a glucose normalization phase [36]. Figure 4 shows an illustrative example of the observer performance against clinical data for a sample patient. As a comparator, the use of a population model for insulin prediction

is considered, since it is still a common practice despite the expected variability in insulin pharmacokinetics (see Section "The subcutaneous insulin route"). With regard to variability, different scenarios are devised: natural physiological variability in insulin pharmacokinetics at a given infusion site along the lifetime of the infusion set; and more abrupt changes in insulin pharmacokinetics due to the use of a new infusion site after rotation, with different subcutaneous tissue properties (for instance, affected by lypohypertrophia [18]). Due to the limited duration of the data (5 hours), the above scenarios are characterized in [35] through the observer initialization, since a change in infusion site is expected to imply a larger mismatch between the observer model and the actual behavior. Thus three cases are compared in Figure 4: (i) a population model is used as insulin predictor considering nominal pharmacokinetic parameters in the Hovorka model, which are clearly detuned for this patient (comparator); (ii) pharmacokinetic parameters k_e and t_{maxI} are included into the Kalman filter for real-time estimation with initial conditions set to nominal parameters in Hovorka model, far from the actual values (representing the case of a new infusion site); and (iii) is the same case as (ii), but initial conditions of the pharmacokinetic parameters are set to the average of the parameter values estimated for the rest of patients (following a cross-validation procedure), which are closer to the actual values as demonstrated by data (representing performance against variability of the current infusion site along its lifetime, after a longer run of the observer). Remark that from the practical perspective, at most only individual parameters may be available for the initialization of pharmacokinetic parameters. Figure 4 shows how real-time estimation of pharmacokinetic parameters leads to the detection of significant deviations in plasma insulin prediction with the population model, reaching more accurate estimations after a transient time (solid blue line). Impact of this transient time on closed-loop performance needs to be investigated. Once adapted, insulin estimation is expected to remain accurate enough (solid green line). Root mean square error (RMSE) and mean absolute relative deviation (MARD) are computed for the assessment of the observer performance in the cohort of patients. The obtained RMSE values are 24.5 ± 16.5 mU/L for case (i), 14.9 ± 7.7 mU/L for case (ii) and 6.6 ± 3.9 mU/L for case (iii). Consideration of the pharmacokinetic parameters k_e and t_{maxI} as extended states significantly improves estimation accuracy, with a reduction of RMSE in 73% with respect to a population model approach.

In the simulation study presented in [37], the Unscented Kalman Filter (UKF) is used to calculate the bolus insulin size based on a state estimate (which includes plasma insulin) and the meal size announced by the patient. The rationale is that aside meal size announcement, information provided by the early postprandial period can help to reduce the impact of errors in carbohydrate counting by the patient, allowing for the computation of more accurate insulin bolus doses even at the expense of a delayed administration. The Identifiable Virtual Patient (IVP) glucose-insulin model [28], described in Section "Glucose-insulin models" and Table 1,

is used in this work. Insulin sensitivity and the meal compartment are also estimated via a state extension. Different bolus administration strategies are investigated (at mealtime, 15 minutes after and 30 minutes after the beginning of the meal) for 10 patients for three-day simulations with three meals per day checking the median time spent in hyperglycemia, within target and in hypoglycemia. No specific results on the observer performance are reported. They conclude that administering the meal bolus 15 minutes after mealtime both reduces the risk of hypoglycemia when meal size is overestimated by 50%, and the time spent in hyperglycemia for a meal size underestimation again by 50%. However, administration of insulin at mealtime is optimal when the meal size is exactly known. Due to the problem posed in this work, administration before the meal is not considered. However, clinical trials that assessed the best timing for meal bolus times generally conclude that the administration of the insulin bolus between 10 to 20 minutes before the meal leads to reduced glycemic excursions, as compared to mealtime or after the meal [38], [39].

Other works address the design of insulin observers but either an intravenous route is considered, not used in current artificial pancreas systems, or endogenous insulin secretion is included, which does not apply to type 1 diabetes. However, these works are reviewed below since they deal with glucose-insulin models and may be relevant to future developments in the artificial pancreas context.

A reduced-order Luenberger observer [40] is designed in [41] for the three-state minimal Bergman model [22], where endogenous insulin secretion in the original model is substituted by an intravenous insulin infusion to represent subjects with type 1 diabetes. Disturbances are included in the form of an exogenous glucose infusion rate. The observer aims at the reconstruction of the remote insulin compartment and plasma insulin deviation from plasma glucose deviation measurements. The obtained results are tested on nonlinear closed loop simulations using the disturbance rejection Linear Quadratic method. A standard meal disturbance with about six-hour duration is considered as test case. Graphically it is shown that the observer is faster than the system itself and it can provide a very good state recovery performance.

In [42] the Bergman Model is used in combination with different filters (symmetric UKF, EKF, simplex UKF and Particle Filter) for the estimation of plasma insulin concentration. Endogenous insulin secretion is considered. Furthermore, linear interpolation is used to obtain glucose measurements in a time grid of 1 minute. After evaluating observability by the Lie derivatives, the designed observers are validated with data from an intravenous glucose tolerance test (IVGTT) (see Section “Glucose-insulin models”) in non-diabetic subjects by computing the root mean square error (RMSE). The symmetric UKF showed better results with an RMSE value of 10.277 mU/L, followed by EKF with 13.533 mU/L. This work is extended later in

[43] to incorporate parameter estimation via state extension characterizing first- and second-phase insulin response as well as compartments for glucose and subcutaneous insulin inputs and for subcutaneous glucose measurements. Both the observability of states and external inputs and the identifiability of model parameters are analyzed by the empirical observability Gramian from data. For the purpose of model validation, four scenarios are simulated: an IVGTT for non-diabetic subjects, an oral glucose tolerant test (OGTT) for non-diabetic subjects, an IVGTT for diabetic subjects and an IVGTT with an insulin bolus after 30 min for diabetic subjects. Similarly to IVGTT, the OGTT is a clinical test to analyze glucose metabolism but glucose is administered orally instead of intravenously. Simulated scenarios are compared with measured data from non-diabetic and diabetic pigs. These data are used for parameter identification and model adaptation. The results are graphically evaluated concluding that a real-time estimation of states, such as plasma insulin, and parameters, such as second-phase insulin response gain, is possible. It may improve real-time state prediction and a personalized model.

In [44], Bergman model is used with the UKF, the cubature quadrature Kalman filter (CQKF) and Gauss-Hermite filter (GHF) to track plasma glucose, plasma insulin and interstitial insulin levels. The authors are based on the work presented in [42]. Thus, endogenous insulin secretion is again considered. The above filters are compared based on estimation accuracy, in terms of RMSE, and computation efficiency by simulation. They show that all three filters successfully trace glucose and insulin levels from noisy blood glucose measurements with similar performances (RMSE plots overlap) but the UFK computational load is lower.

Finally, in [45], [46], [47], nonlinear discrete-delay differential equation (DDE) models are used in the context of closed-loop glucose control. The authors state that DDE models seem to represent better the pancreatic insulin delivery rate, allowing for the extension of the methodologies to type 2 diabetes. Moreover, the model has satisfactory properties, such as positivity and boundedness of solutions or local attractivity of a single positive equilibrium. It is as well statistically robust, since its parameters are identifiable with very good precision by means of standard perturbation experiments, such as IVGTT. The authors consider the problem of tracking a desired plasma glucose trajectory from initial hyperglycemia making use of only glucose measurements. To this aim, they use the nonlinear observer for time-delay systems to estimate the plasma insulin concentration

$$\begin{bmatrix} \frac{\hat{G}(t)}{dt} \\ \frac{\hat{I}(t)}{dt} \end{bmatrix} = \begin{bmatrix} -K_{xgi}\hat{G}(t)\hat{I}(t) + \frac{T_{gh}}{V_G} \\ -K_{xi}\hat{I}(t) + \frac{T_{iGmax}}{V_I} f(\hat{G}(t-\tau_g) + \frac{u(t)}{V_I}) \end{bmatrix} + Q^{-1}(\hat{G}(t), \hat{I}(t))W(G(t) - \hat{G}(t)), \tag{7}$$

where $\hat{G}(t)$ and $\hat{I}(t)$ denote the glucose and insulin estimates, respectively, and Q^{-1} is the inverse

matrix of the matrix function

$$Q(x_1, x_2) = \begin{bmatrix} 1 & 0 \\ -K_{xgi}x_2 & -K_{xgi}x_1 \end{bmatrix}. \tag{8}$$

The observer gain matrix $W \in \mathbb{R}^{2\times 1}$ is designed to ensure that

$$\hat{H} = \begin{bmatrix} 0 & 1 \\ 0 & 0 \end{bmatrix} - W \begin{bmatrix} 1 & 0 \end{bmatrix}$$

is Hurwitz with prescribed eigenvalues in the left half complex plane.

Numerical results from simulations show that this approach is robust with respect to the uncertainties of the model parameters, as well as to the glucose measurement errors and insulin pump malfunctioning.

Table 2 summarizes the above results.

Insulin infusion limitation in the artificial pancreas

As previously stated, the main justification for the prediction, or estimation from data, of plasma insulin or insulin-on-board in an artificial pancreas is the avoidance of the controller's over-actuation (for instance, after a meal disturbance) inducing an excessive insulin infusion with the consequent risk of hypoglycemia. Model predictive control (MPC), proportional-integral-derivative (PID) and fuzzy logic (FL) are the major control strategies used in the artificial pancreas framework and most extensively evaluated through clinical trials [48]. According to a recent review [49], 18 artificial pancreas systems are currently under development at different stages, of which eight are based on MPC, six on a PID-type control algorithm, three on FL and one in a bio-inspired approach. All of them must deal with the limitation of insulin infusion for the sake of safety. Their strategies are reviewed next.

Model Predictive Control

One of the advantages of MPC control is that it can easily incorporate constraints into the optimization process of the defined cost function. An example of such procedure is given in [50] where a dynamic safety constraint on the maximum rate of insulin delivery based on empirical clinical knowledge is integrated into an MPC control scheme in order to avoid over-delivery of insulin. The following constrained cost function is considered

$$\min_{u\in\mathbb{R}} \left(\omega_y \hat{\mathbf{y}}^{\mathbf{T}}\hat{\mathbf{y}} + \omega_u \hat{\mathbf{u}}^{\mathbf{T}}\hat{\mathbf{u}} + \omega_{\Delta u}\boldsymbol{\Delta}\mathbf{u}^{\mathbf{T}}\boldsymbol{\Delta}\mathbf{u}\right), \tag{9}$$

s.t.

$$-0.5\hat{\mathbf{u}}_{\mathbf{ss}} \leq \hat{\mathbf{u}} \leq U_{max}(k), \tag{10}$$

where $\hat{\mathbf{y}} \in \mathbb{R}^{p\times 1}$ is the vector of predicted plasma glucose deviations with respect to the glucose setpoint, with p the output prediction horizon; $\hat{\mathbf{u}} \in \mathbb{R}^{m\times 1}$ is the vector of future calculated deviations of insulin infusion rate with respect to the basal rate $\hat{\mathbf{u}}_{\mathbf{ss}}$ (that is, the insulin rate required at steady-state to obtain the desired steady-state glycemia), with m the control horizon; and $\mathbf{\Delta u} \in \mathbb{R}^{m\times 1}$ is the vector of future insulin infusion increments. The constraint, expressed in terms of deviations of insulin infusion rate with respect to the basal rate $\hat{\mathbf{u}}_{\mathbf{ss}}$, indicates that insulin infusion rate is limited between half its basal value and a time-dependent maximum deviation from its basal value, $U_{max}(k)$, given by

$$U_{max}(k) = \begin{cases} I_{CHO}(k) + I_G(k) - IOB(k) & \text{if } I_{CHO}(k) + I_G(k) > IOB(k) \\ I_{CHO}(k) & \text{otherwise} \end{cases}, \tag{11}$$

with

$$I_{CHO}(k) = M(k) \cdot IC, \tag{12}$$

$$I_G(k) = \begin{cases} (G(k) - G_{ss}(k)) \cdot CF & \text{if } G(k) - G_{ss}(k) > 0 \\ 0 & \text{otherwise} \end{cases}, \tag{13}$$

where $I_{CHO}(k)$ is the insulin needed at time k to compensate a meal, $M(k)$ is the amount of carbohydrates from the meal absorbed at time k and IC [U/g] the insulin-to-carbohydrate ratio used currently by clinicians (that is, how much insulin per gram of carbohydrate must be administered to compensate a meal). Moreover, $I_G(k)$ represents the insulin needed to compensate a deviation from target (considered here the steady-state glucose concentration), $G_{ss}(k)$, as given by the correction factor CF [U (mg/dL)$^{-1}$] used by clinicians in current insulin therapy (that is, how much insulin must be administered to compensate an excess of one glucose concentration unit with respect to glucose target).

Finally, $IOB(k)$ is the predicted insulin-on-board at time k, which is obtained from the convolution of the insulin administered in the last eight hours and a family of "active insulin curves" as given by insulin pump manufacturers ranging different durations of insulin action (DIA) from 2 to 8 hours. These curves are based on insulin action plots and express the percentage of remaining active insulin along time. Curvilinear and linear versions are available, depending on the manufacturer [51]. Although linear versions are easier to use by patients, curvilinear versions represent better subcutaneous insulin pharmacokinetics and they are preferred. The use of dynamic curves to account for daily variations in insulin sensitivity is proposed in [52].

In a simulation study reproducing a 24h clinical protocol with three meals [50], limitation of IOB according to (9)-(10) resulted in a reduction of the number of simulations yielding a hypoglycemic event, compared to the same MPC controller without IOB constraint, from 50% (18.6% of the overall simulation time) to 10% (0.75% of the overall simulation time). This

was achieved at the expense of mild hyperglycemia, but for very short periods (3.5% of overall simulation time).

In [53], the insulin limitation problem is casted into an augmented single-input multiple-output MPC formulation where the linear combination

$$\Phi(t) := s_I I(t) + s_q q(t) \tag{14}$$

of plasma insulin, $I(t)$, and a measure of the pending effect of insulin-on-board, $q(t)$, is added as a new system output. A generalized predictive control (GPC) with extended output $\mathbf{y}(t) := [G(t)\ \Phi(t)]^T$ ($G(t)$ is plasma glucose), is then formulated. GPC optimizes the multi-stage quadratic cost function, after signals discretization,

$$J_{GPC} = \sum_{k=N_d}^{N_m} \delta_k \|\mathbf{C}(\mathbf{r}_{t+k} - \mathbf{y}_{t+k})\|^2 + \sum_{k=0}^{N_u} \lambda_k (\Delta u_{t+k})^2, \tag{15}$$

where the first term penalizes the error with respect to the setpoint $\mathbf{r}$ along the prediction horizon $[N_d, N_m]$ and the second term penalizes the control action along the control horizon with bound N_u. Parameters δ_k and λ_k are weights.

In this case, the following bi-exponential insulin pharmacokinetic model is used

$$I(t) = KU_0 \left(e^{-\alpha_1 t} - e^{-\alpha_2 t}\right), \tag{16}$$

which corresponds to (2) with $K := \frac{1}{K_{cl}(\tau_2 - \tau_1)}$, $\alpha_1 := \frac{1}{\tau_2}$ and $\alpha_2 := \frac{1}{\tau_1}$. The pending effect of insulin-on-board at time t is computed as

$$q(t) = \int_t^\infty I(\tau) d\tau = \frac{KU_0}{\alpha_1 \alpha_2} \left(\alpha_2 e^{-\alpha_1 t} - \alpha_1 e^{-\alpha_2 t}\right). \tag{17}$$

Factors s_{Ip} and s_q in equation (14) scale the corresponding units of $I(t)$ [U/dL] and $q(t)$ [Umin/dL] into [mg/dL] for an homogeneous cost index. Remark that $q(t)$ is an area-under-the-curve of plasma insulin concentration, not mass of insulin.

Finally, another relevant MPC-based artificial pancreas system is presented in [23], already tested in free living conditions without supervision during three months [54]. Their system includes the following safety checks to avoid excess of insulin delivery [31]: (i) insulin infusion rate is limited of 2 to 5 times the preprogrammed basal rate, depending on the current glucose measurement, the time since the previous meal(s), and carbohydrate content of meal(s); (ii) shutting off insulin delivery when glucose measurement is below 77 mg/dL; (iii) reducing insulin delivery when glucose is decreasing rapidly; and (iv) capping the insulin infusion to the preprogrammed basal rate if a pump occlusion is inferred by the MPC. Unfortunately no more technical details were published aside the ones presented here extracted from their patent, to the best of our knowledge.

PID Control

Two approaches with clinical validation are found for insulin limitation in PID-based artificial pancreas systems: Insulin Feedback and Sliding Mode Reference Conditioning. Although applied to PID control, they might be used with other control structures.

Insulin feedback

In a healthy person, the beta cells do automatically avoid insulin excess by auto-inhibiting the endogenous insulin production depending on the insulin plasmatic concentration. However, in type 1 diabetes this phenomenon is lost due to the destruction of the auto-regulating beta cells. However, an artificial pancreas can emulate this process by using the Insulin Feedback algorithm (IFB) [55], where a prediction of plasma insulin is fed on the forward delivery of insulin of the PID algorithm. All PID-based studies used this strategy since then [48], with just one exception that is reviewed in the next section [56].

The classic PID control within the artificial pancreas framework usually include the following three different terms

$$u_{AP} = u_{PID} + u_{basal} + u_{bolus}, \tag{18}$$

where u_{basal} is the basal insulin needed by the patient to keep a proper glycemia level between meals and at night (basal metabolic conditions), u_{PID} is the additional control action (insulin delivered) proposed by the PID algorithm to deal mainly with disturbances, and u_{bolus} is the extra insulin dose needed at meal time (considering meal announcement, where the patient informs the control algorithm about the meal time and estimated amount of carbohydrates).

A possible implementation of the IFB algorithm (see [30] or [29]) is

$$u_{IFB} = u_{AP} - \gamma I, \tag{19}$$

where the original control action u_{AP} is limited by an action proportional to the predicted plasma insulin concentration I. For this purpose, the bi-exponential model (2) is used, with transfer function given by

$$G_{PK_{IFB}}(s) := \frac{I(s)}{u_{IFB}(s)} = \frac{\frac{1}{\tau_1}\frac{1}{\tau_2}}{K_{cl}(s+\frac{1}{\tau_1})(s+\frac{1}{\tau_2})}, \tag{20}$$

which corresponds to equation (1) with input signal u_{IFB}. The γ parameter multiplying I must be set by the control engineer. The insulin feedback approach described is, from a classical control point of view, mathematically equivalent to a cascade control system [30], as shown in Figure 5. It must be remarked that for IFB to keep the original insulin infusion u_{AP} at steady

state, the original PID parameters must be retuned or a reduction in insulin infusion would lead to an increase in glucose concentration [30]. In order to avoid this, the term u_{AP} in (19) must be multiplied by $f := (1 + \gamma \lim_{s\to 0} G_{PK_{IFB}}(s))$. This is equivalent to retuning the controller's proportional gain. Integral and derivative terms may also need some adjustments depending on the tuning of γ.

Equation (21) presents an equivalent IFB implementation as a limiting action proportional to $I - I_B$, where I_B is the predicted basal plasma insulin:

$$u_{IFB} = u_{AP} - \gamma \left(I - I_B\right). \tag{21}$$

In this case the additional term is zero in basal (stationary) conditions and PID gain retuning is thus not necessary.

Different studies show the good performance of the IFB approach. In [30] simulation results using the Hovorka model [23] are presented for 24h with 3 meals, and a decrement of the peak postprandial excursion while at the same time a reduction of late-postprandial hypoglycemia is reported. In [55], the ability of IFB to improve the breakfast meal profile in a 30h closed-loop in-clinic study with 8 adult subjects with type 1 diabetes was assessed with a substantial improvement over prior studies, but supplemental carbohydrates after breakfast was needed for 3 subjects; the clinical study also showed feasibility of overnight control. On the other hand, in [57] 4 subjects were studied for 24h and the IFB, as compared to a standard PID control, reduced the occurrence of hypoglycemia without increasing meal-related glucose excursions. Finally, [58] presents simulation results of the IFB strategy used in a fully implantable artificial pancreas using intraperitoneal insulin delivery and glucose sensing (that is, the peritoneal cavity, which is the area in the body that contains the abdominal organs, is used for a rapid sensing and actuation, mimicking better the healthy pancreatic activity). In this case, the IFB alone was not enough to attenuate postprandial undershoot but in combination with anti-windup provided very good results.

Sliding Mode Reference Conditioning control

The technique of Sliding Mode Reference Conditioning (SMRC) is proposed in [56] to build an external feedback loop, named as Safety Auxiliary Feedback Element (SAFE), in order to keep "insulin-on-board", represented here by the size of the subcutaneous insulin depot, inside predefined limits. Remark that this measure differs from the "active insulin curves" currently used in insulin pumps which include insulin pharmacodynamics [59]. Upper and lower limits for IOB can be defined if desired. SMRC uses the modulation of glucose target as a new degree of freedom for glucose regulation (see Figure 6). A prediction of insulin-on-board, $IOB(t)$,

drives a switching function $\sigma_{SM}(t)$ triggering a discontinuous signal $\omega(t)$ that, after a filtering step, adds up to the standard glucose target. The rationale behind SMRC is that a way to upper limit insulin-on-board is by increasing the desired glucose target. Any controller will react in the sought direction: diminishing insulin infusion. The opposite applies when a lower limit for insulin-on-board is desired.

SMRC originates on concepts of invariance control and sliding regimes as a transitional mode of operation. In contrast with conventional sliding mode control, the aim here is not evolving in sliding regime towards the equilibrium point. Only when the system, by itself, reaches a given sliding surface separating the space into feasible and unfeasible regions (characterized by the constraint on insulin-on-board in this case), the sliding regime is stablished by conditioning the reference, until the system returns, by itself again, to the feasible region. In this sense, there is no reaching mode as such, since no control effort is done to drive the system to the sliding surface [60].

Given a (possibly time-variant) upper limit on insulin-on-board, $\overline{IOB}(t)$, and denoting as $x(t)$ the system state, the set

$$\Sigma := \left\{ x(t) \mid IOB(t) \leq \overline{IOB}(t) \right\} \tag{22}$$

is invariant (that is, if the initial state fulfills the constraint $IOB(t) \leq \overline{IOB}(t)$, then it will be fulfilled for all $t > 0$) for a discontinuous signal $\omega(t)$ of the form

$$\omega(t) = \begin{cases} \omega^+ & \text{if } \sigma_{SM}(t) > 0 \\ 0 & \text{otherwise} \end{cases}, \tag{23}$$

with $\omega^+ > 0$ large enough (see [56] for technical details) and

$$\sigma_{SM}(t) := IOB(t) - \overline{IOB}(t) + \sum_{i=1}^{l-1} \tau_i \left(IOB(t)^{(i)} - \overline{IOB}(t)^{(i)} \right), \tag{24}$$

where l is the relative degree between the output $IOB(t)$ and the input $\omega(t)$, superscript (i) denotes the i-th derivative and τ_i are constant gains.

The first-order filter

$$\frac{dG_{RF}(t)}{dt} = -\alpha G_{RF}(t) + \alpha(G_R(t) + \omega(t)) \tag{25}$$

is considered to keep all signals in the control loop smooth, where $G_{RF}(t)$ is the modulated (conditioned) glucose target fed to the controller, $G_R(t)$ is the standard glucose target (usually constant), and α defines the filter cut-off frequency. Remark that stability of the system is guaranteed since the SMRC loop acts only on the setpoint, which is always bounded.

Relative degree l is determined by the relative degree of the filter (25) and the relative degree of the insulin-on-board predictor, since the controller has a proportional action. Although the subcutaneous insulin pharmacokinetic model in [61] was considered in the initial work [56] (which is the model in the UVA/Padova simulator), the Hovorka subcutaneous insulin pharmacokinetic model [23] (presented in Table 1 and reproduced here for clarity),

$$\frac{dS_1(t)}{dt} = u_{sc}(t) - \frac{1}{t_{maxI}} S_1(t), \tag{26}$$

$$\frac{dS_2(t)}{dt} = \frac{1}{t_{maxI}} (S_1(t) - S_2(t)), \tag{27}$$

with insulin-on-board defined as

$$IOB(t) := S_1(t) + S_2(t), \tag{28}$$

was finally chosen in the implementation for clinical evaluation due to parsimony criteria. Figure 7 shows the typical time profile of insulin-on-board as defined by (26)-(28) expressed as a percentage of the bolus size. It becomes apparent the curvilinear nature of subcutaneous insulin pharmacokinetics, also characteristic of active insulin curves provided by insulin pump manufacturers [51].

Model (26)-(28) has a relative degree of 1, giving rise to a total relative degree of $l = 2$. The switching function (24) is thus given by

$$\sigma_{SM}(t) = IOB(t) - \overline{IOB}(t) + \tau \left(\frac{dIOB(t)}{dt} - \frac{d\overline{IOB}(t)}{dt} \right). \tag{29}$$

For an interpretation of the above switching function, consider, for simplicity, a constant upper IOB limit, $\overline{IOB}$. This will be so, for instance, in a postprandial period or during the night. The switching function $\sigma_{SM}(t)$ will be positive when $IOB(t) + \tau \frac{dIOB(t)}{dt}$ exceeds the limit $\overline{IOB}$, that is, when the predicted IOB is "about" to violate the constraint. How close IOB is allowed to approach (from below) its limit will depend on the IOB trend, weighted by the tuning parameter τ. This defines a threshold on IOB, which corresponds to $\overline{IOB} - \tau \frac{dIOB(t)}{dt}$. A rapidly changing IOB will lower this threshold compared to an IOB approaching slowly the limit. A similar interpretation holds for variable upper IOB limit, $\overline{IOB}(t)$, but in this case the threshold on IOB depends on the difference in the trends for IOB and its limit. When IOB goes beyond this threshold, an increment of the glucose setpoint is triggered, provoked by the discontinuous signal $\omega(t)$ and amounting to ω^+, after a transient given by the filter (25). As a reaction to the new (generally much higher) glucose setpoint, the controller will reduce the insulin delivery, impeding the violation of the IOB limit for high enough ω^+. Glucose setpoint will return to its original value, after the transient imposed by the filter, when IOB goes back below the threshold in which case $\omega(t) = 0$.

Similar formulae are obtained for lower limiting insulin-on-board, changing the inequality sense in (23) and the sign for $\omega(t)$ (glucose target must be decreased).

SMRC was evaluated, in combination with a PD controller, in an in-clinic clinical study where 20 patients with type 1 diabetes underwent a standardized 60g-carbohydrate mixed meal on four occasions (two in open loop and two in closed loop). SMRC showed an improvement of postprandial control with a significant decrement of postprandial peak and increment of time-in-range (70-180mg/dL) without a clinically meaningful increased risk of hypoglycemia [62]. Simulation validation of SMRC in combination with other controllers can be found in [63] demonstrating the benefit of the SAFE loop.

Fuzzy Logic

The two control strategies presented previously (MPC and PID) are based on the use of mathematical models of glucose-insulin dynamics. However, the biological system to be controlled is nonlinear and complex, and subject to lags and uncertainties. Therefore, it is very difficult to capture the physiological behavior of a patient. Fuzzy logic allows the development of a fuzzy controller without any patient model by including fuzzy rules (IF input is A THEN output is B), where A and B are linguistic variables. In this way, a controller can be built from medical expertise [64]. In addition, multiple inputs and multiple outputs can be included in a natural way. Different groups have proposed a fuzzy-controller-based artificial pancreas [65], [66], and insulin limitation based on predictions of insulin-on-board are also applied in fuzzy logic systems.

The MD-logic system presented in [65] is based on: (i) a control-to-range layer consisting on fuzzy rules giving rise to an insulin recommendation expressed as percentage of patient's basal insulin; and (ii) a control-to-target layer that takes into account, among other things, special glucose dynamics requiring specific corrections and safety measures. The control-to-range layer considers four inputs: past and future glucose trend, and current and future glucose level. This latter is predicted through an auto-regressive model. The values of the trend input variables are defined as "steep descent", "descent", "stable", "ascent" and "steep ascent", defined over the range of $\pm$ 5 mg/dL/min. Glucose level values are defined as "very low", "low", "normal", "normal high", "high" and "very high", defined over the physiological range for glucose. Two output variables are considered: percent change in patient's standard basal rate and standard bolus. In the control-to-target layer, the final insulin rate to be delivered in computed. A prediction of insulin-on-board based on the following piecewise functional approximation of insulin aspart

pharmacokinetics is considered [7]

$$f_{I/G}[\%] = \begin{cases} 1 & t \leq t_1 \\ P_2 & t_1 < t \leq t_2 \\ \frac{P_3(t-t_3)}{t_3-t_2} & t_2 < t \leq t_3 \\ 0 & t_3 < t \end{cases}, \tag{30}$$

and subtracted from the insulin to be delivered (see Supplemental data in [65]). Unfortunately no further technical details are provided.

Another fuzzy logic approach is the Dose Safety system presented in [66], [67]. The fuzzy controller has as well two components: (i) the fuzzy logic Dosing component, which computes through a rule matrix an insulin dose based on the glucose value, rate and acceleration to keep glucose in the range 80-120 mg/dL; and (ii) the Dosing Personalization component, which computes a personalization scale factor for the computed insulin dose. In [66], it is stated that the system does not track insulin-on-board, although the function will be included in subsequent versions. In [68] an extension of the system with a Hypoglycemia Prevention Module is presented, which incorporates a hypoglycemia predictor based on pattern matching techniques from glucose and insulin-on-board signals. However, to the best of our knowledge, no further technical details have been disclosed.

Open challenges

The use of the artificial pancreas in free living conditions poses extra challenges to the performance of the controller, and with it, the efficiency of its mechanisms for insulin infusion limitation. An example is physical activity, with very different effects on plasma glucose concentration depending on its type and intensity. Mild and moderate intensity physical activity requires a reduction of insulin infusion, while more intense activities necessitate a rise in insulin, at least in early recovery [69]. This can affect algorithms limiting insulin infusion under physical activity scenarios, which may need a different tuning. However, it implies that the system must be informed in some way about physical activity, such as patient's announcement or measurements from a physical activity monitor.

Moreover, the dynamic lags imposed by the subcutaneous route might be a barrier for an efficient compensation of physical activity, which may provoke rapid fluctuations in glucose. Subcutaneous insulin pharmacokinetics can also be affected by physical activity. In [70], an increase of circulating insulin is observed after a pump basal insulin rate reduction before a moderate-intensity aerobic exercise, which is hypothesized to be due to the increased cardiac output and increased subcutaneous blood flow during exercise provoking an acceleration of

insulin pharmacokinetics. It is thus expected that physical activity may affect the performance of insulin observers. To date, there are no accurate enough exercise models. Physical activity can also compromise accuracy of continuous glucose measurements, with an overall overestimation of glucose values [71]. Possible sources of this loss of performance are changes in subcutaneous blood circulation and increase in body and skin temperature during physical activity, which affect the dynamics of glucose transport between plasma and the interstitial space where the sensor is located.

Another important challenge is postprandial control. There is growing evidence that insulin dosing algorithms should consider not only the carbohydrate content of a meal, but also fat and protein [72], [73], [74]. An artificial pancreas study investigating performance for a low-fat versus high-fat dinner, with identical carbohydrate content, showed elevated plasma glucose levels during the high-fat dinner despite the administration of 42% more insulin [75]. Model fitting from data produced in this study revealed not only the expected lag in gastric emptying due to an increased fat content, but also a lower insulin sensitivity in the high-fat meal [73]. In [74], a controlled study was conducted comparing a low-fat-low-protein meal with a high-fat-high-protein meal with identical carbohydrate content, covered with identical insulin doses, showing a two-fold glucose incremental area under the curve in the latter case. In the same study, an adaptive model-predictive insulin bolus strategy required 65% more insulin, with a 30%/70% split over 2.4h, to achieve glucose target in the high-fat-high-protein case, compared to low-fat-low-protein. Further investigation is needed to understand how these findings affect the performance of insulin limitation algorithms in an AP. Meal composition announcement is not desirable due to the extra burden for patients. Besides, current meal models only consider carbohydrates which is an important limitation.

The need to incorporate psychological stress into the artificial pancreas is also under investigation. In [76], a significant relationship between daily stress (rated by the patient in a 5-point scale) and glucose variability was found, as well as an increase percentage of time in hypoglycemia and reduced carbohydrate consumption. However, mean glucose was not affected. More studies are needed to reveal the clinical significance of these findings and justify its consideration in an artificial pancreas for individuals more reactive to stress.

As more data is available from long-term clinical closed-loop studies in free living conditions, improvements addressing all these aspects may be expected.

Conclusion

Glucose control in type 1 diabetes is a complex problem from the control engineering point of view. The plant (that is, the patient) is a highly-variant nonlinear system due to the nature of physiology and its intrinsic variability. Besides, significant lags are introduced by the use of the subcutaneous route, due to its minimal invasiveness. The fact that insulin has a unidirectional action poses additional challenges to the efficacy and safety of control algorithms. These aspects were introduced in this article, focusing both on physiological knowledge for a thorough understanding of the problem at hand, and different control engineering approaches proposed in the artificial pancreas field to address these challenges.

It becomes apparent that a critical component of any artificial pancreas is the limitation of insulin delivery based on some measure of insulin in the body. Plasma insulin concentration, active insulin curves and size of the subcutaneous insulin depot are examples of such measures. Methods for insulin limitation differ depending on the control framework. MPC incorporates such measures as constraints or in the cost index for optimization. PID control makes use of additional structures such as cascade control or reference conditioning. Fuzzy logic incorporates insulin measures as components of the rule base. All these approaches are based on insulin predictors (or estimators). Due to the large variability, another critical component of an artificial pancreas shows to be real-time estimation and model parameters adaptation. The availability of continuous glucose measurements allows to address this problem through the design of observers. Different observer techniques have been used to this purpose, although validation with clinical data is scarce. Results published on the development of insulin observers were reviewed. Some open challenges were also pointed out. With this, this article aims at introducing the reader in the challenge of automatic subcutaneous insulin delivery and the opportunities that it brings to control engineering to alleviate the current burden of self-control to patients with type 1 diabetes.

Acknowledgements

This work was supported by the Spanish Ministry of Economy and Competitiveness (MINECO) through grant DPI2013-46982-C2-1-R and the EU through FEDER funds.

References

[1] B. Kovatchev, W. V. Tamborlane, W. T. Cefalu, and C. Cobelli, "The Artificial Pancreas in 2016: A Digital Treatment Ecosystem for Diabetes," *Diabetes Care*, vol. 39, pp. 1123–1126, 2016.

[2] Food and Drug Administration (FDA), "The Artificial Pancreas Device System," http://www.fda.gov/medicaldevices/productsandmedicalprocedures/homehealthandconsumer/consumerproducts/artificialpancreas/default.htm, 2016, [Online; accessed 30-Oct-2016].

[3] R. Hovorka, "Continuous glucose monitoring and closed-loop systems," *Diabetic Medicine*, vol. 23, no. 1, pp. 1–12, 2006.

[4] E. Renard, J. Place, M. Cantwell, H. Chevassus, and C. C. Palerm, "Closed-Loop Insulin Delivery Using a Subcutaneous Glucose Sensor and Intraperitoneal Insulin Delivery: Feasibility study testing a new model for the artificial pancreas," *Diabetes care*, vol. 33, no. 1, pp. 121–127, 2009.

[5] J. Pickup and H. Keen, "Continuous subcutaneous insulin infusion at 25 years: evidence base for the expanding use of insulin pump therapy in type 1 diabetes," *Diabetes care*, vol. 25, no. 3, pp. 593–598, 2002.

[6] L. Heinemann and L. Krinelke, "Insulin infusion set: the Achilles heel of continuous subcutaneous insulin infusion," *Journal of Diabetes Science and Technology*, vol. 6, no. 4, pp. 954–964, 2012.

[7] S. R. Mudaliar, F. A. Lindberg, M. Joyce, P. Beerdsen, P. Strange, A. Lin, and R. R. Henry, "Insulin aspart (B28 asp-insulin): a fast-acting analog of human insulin: absorption kinetics and action profile compared with regular human insulin in healthy nondiabetic subjects," *Diabetes care*, vol. 22, no. 9, pp. 1501–1506, 1999.

[8] F. Holleman and J. Hoekstra, "Insulin lispro," *New England Journal of Medicine*, vol. 337, no. 3, pp. 176–183, 1997.

[9] C. Homko, A. Deluzio, C. Jimenez, and J. Kolaczynski, "Comparison of Insulin Aspart and Lispro Pharmacokinetic and metabolic effects," *Diabetes care*, vol. 26, pp. 2027–2031, 2003.

[10] J. Brange and A. Vølund, "Insulin analogs with improved pharmacokinetic profiles," *Advanced Drug Delivery Reviews*, vol. 35, pp. 307–335, 1999.

[11] L. Ranganath, F. Schaper, R. Gama, and L. Morgan, "Mechanism of glucagon-induced nausea," *Clinical endocrinology*, vol. 51, no. 2, pp. 260–261, 1999.

[12] A. J. Kowalski, "Can we really close the loop and how soon? Accelerating the availability of an artificial pancreas: a roadmap to better diabetes outcomes," *Diabetes Technology & Therapeutics*, vol. 11 Suppl 1, pp. S113–9, 2009.

[13] A. Haidar, D. Elleri, K. Kumareswaran, L. Leelarathna, J. M. Allen, K. Caldwell, H. R.

Murphy, M. E. Wilinska, C. L. Acerini, M. L. Evans, D. B. Dunger, M. Nodale, and R. Hovorka, "Pharmacokinetics of insulin aspart in pump-treated subjects with type 1 diabetes: reproducibility and effect of age, weight, and duration of diabetes." *Diabetes care*, vol. 36, no. 10, pp. e173–e174, 2013.

[14] L. Heinemann, "Variability of insulin absorption and insulin action," *Diabetes Technology & Therapeutics*, vol. 4, no. 5, pp. 673–682, 2002.

[15] G. Scheiner and B. Boyer, "Characteristics of basal insulin requirements by age and gender in Type-1 diabetes patients using insulin pump therapy," *Diabetes Research and Clinical Practice*, vol. 69, pp. 14–21, 2005.

[16] M. C. Jolly, R. Hovorka, I. Godsland, R. Amin, N. Lawrence, V. Anyaoku, D. Johnston, and S. Robinson, "Relation between insulin kinetics and insulin sensitivity in pregnancy." *European Journal of Clinical Investigation*, vol. 33, no. 8, pp. 698–703, 2003.

[17] O. U. Petring and H. Flachs, "Inter- and intrasubject variability of gastric emptying in healthy volunteers measured by scintigraphy and paracetamol absorption," *British Journal of Clinical Pharmacology*, vol. 29, no. 6, pp. 703–708, 2012.

[18] S. Famulla, U. Hövelmann, A. Fischer, H.-V. Coester, L. Hermanski, M. Kaltheuner, L. Kaltheuner, L. Heinemann, T. Heise, and L. Hirsch, "Insulin Injection Into Lipohypertrophic Tissue: Blunted and More Variable Insulin Absorption and Action, and Impaired Postprandial Glucose Control." *Diabetes care*, 2016.

[19] L. Heinemann, L. Hirsch, and R. Hovorka, "Lipohypertrophy and the artificial pancreas: is this an issue?" *Journal of Diabetes Science and Technology*, vol. 8, no. 5, pp. 915–917, 2014.

[20] C. Cobelli, C. Dalla Man, G. Sparacino, L. Magni, G. De, and B. P. Kovatchev, "Diabetes: Models, Signals, and Control," *IEEE Transactions on Biomedical Engineering*, vol. 2, pp. 54–96, 2009.

[21] C. Cobelli, C. Dalla Man, M. G. Pedersen, A. Bertoldo, and G. Toffolo, "Advancing Our Understanding of the Glucose System via Modeling: A Perspective." *IEEE Transactions on Biomedical Engineering*, vol. 61, no. 5, pp. 1577–1592, Apr. 2014.

[22] R. N. Bergman, L. S. Phillips, and C. Cobelli, "Physiologic evaluation of factors controlling glucose tolerance in man: measurement of insulin sensitivity and beta-cell glucose sensitivity from the response to intravenous glucose," *Journal of Clinical Investigation*, vol. 68, pp. 1456–1467, 1981.

[23] R. Hovorka, V. Canonico, L. J. Chassin, U. Haueter, M. Massi-Benedetti, M. O. Federici, T. R. Pieber, H. C. Schaller, L. Schaupp, T. Vering, and M. Wilinska, "Nonlinear model predictive control of glucose concentration in subjects with type 1 diabetes," *Physiological Measurement*, vol. 25, pp. 905–920, 2004.

[24] C. Dalla Man, R. Rizza, and C. Cobelli, "Meal Simulation Model of the Glucose-Insulin

System," *IEEE Transactions on Biomedical Engineering*, vol. 54, no. 10, pp. 1740–1749, 2007.

[25] C. Dalla Man, F. Micheletto, D. Lv, M. Breton, B. Kovatchev, and C. Cobelli, "The UVA/PADOVA Type 1 Diabetes Simulator: New Features," *Journal of Diabetes Science and Technology*, vol. 8, no. 1, pp. 26–34, Jan. 2014.

[26] R. N. Bergman, Y. Z. Ider, C. R. Bowden, and C. Cobelli, "Quantitative estimation of insulin sensitivity." *American Journal of Physiology – Endocrinology and Metabolism*, vol. 236, no. 6, pp. E667–77, Jun. 1979.

[27] M. E. Wilinska, L. Chassin, C. Acerini, J. M. Allen, D. B. Dunger, and R. Hovorka, "Simulation Environment to Evaluate Closed-Loop Insulin Delivery Systems in Type Diabetes," *Journal of Diabetes Science and Technology*, vol. 4, no. 1, pp. 132–144, 2010.

[28] S. S. Kanderian, S. A. Weinzimer, and G. M. Steil, "The Identifiable Virtual Patient Model: Comparison of Simulation and Clinical Closed-Loop Study Results," *Journal of Diabetes Science and Technology*, vol. 6, no. 2, pp. 371–379, 2012.

[29] G. M. Steil, K. Rebrin, C. Darwin, F. Hariri, and M. F. Saad, "Feasibility of Automating Insulin Delivery for the Treatment of Type 1 Diabetes," *Diabetes*, vol. 55, pp. 3344–3350, 2006.

[30] C. C. Palerm, "Physiologic insulin delivery with insulin feedback: A control systems perspective," *Computer Methods and Programs in Biomedicine*, vol. 102, pp. 130–137, 2011.

[31] M. E. Wilinska, E. S. Budiman, G. A. Hayter, M. B. Taub, and R. Hovorka, "Method of Overnight Closed-Loop Insulin Delivery with Model Predictive Control and Glucose Measurement Error Model," Patent US201 113 240 855, Jan., 2012.

[32] R. Gondhalekar, E. Dassau, H. C. Zisser, and F. J. Doyle III, "Periodic-zone model predictive control for diurnal closed-loop operation of an artificial pancreas." *Journal of Diabetes Science and Technology*, vol. 7, no. 6, pp. 1446–1460, 2013.

[33] R. A. Harvey, E. Dassau, W. Bevier, D. E. Seborg, L. Jovanovic, F. J. Doyle, and H. C. Zisser, "Clinical Evaluation of an Automated Artificial Pancreas Using Zone-Model Predictive Control and Health Monitoring System." *Diabetes Technology & Therapeutics*, vol. 16, no. 6, pp. 348–357, 2014.

[34] J. J. Lee, R. Gondhalekar, and F. J. Doyle, "Design of an artificial pancreas using zone model predictive control with a Moving Horizon State Estimator," in *IEEE 53rd Annual Conference on Decision and Control (CDC), 2014*, 2014, pp. 6975–6980.

[35] D. de Pereda, S. Romero-Vivó, B. Ricarte, P. Rossetti, F. J. Ampudia-Blasco, and J. Bondia, "Real-time estimation of plasma insulin concentration from continuous glucose monitor measurements," *Computer Methods in Biomechanics and Biomedical Engineering*, vol. DOI: 10.1080/10255842.2015.1077234, 2015.

[36] P. Rossetti, F. J. Ampudia-Blasco, A. Laguna, A. Revert, J. Vehí, J. F. Ascaso, and J. Bondia, "Evaluation of a Novel Continuous Glucose Monitoring-Based Method for Mealtime Insulin Dosing—the iBolus—in Subjects with Type 1 Diabetes Using Continuous Subcutaneous Insulin Infusion Therapy: A Randomized Controlled Trial," *Diabetes Technology & Therapeutics*, vol. 14, no. 11, pp. 1043–1052, 2012.

[37] D. Boiroux, T. Aradóttir, M. Hagdrup, N. Poulse, H. Madsen, and J. Jϕrgensen, "A Bolus Calculator Based on Continuous-Discrete Unscented Kalman Filtering for Type 1 Diabetics," *IFAC-PapersOnLine*, vol. 48–20, pp. 159–164, 2015.

[38] E. Cobry, K. McFann, L. Messer, V. Gage, B. VanderWel, L. Horton, and H. P. Chase, "Timing of Meal Insulin Boluses to Achieve Optimal Postprandial Glycemic Control in Patients with Type 1 Diabetes," *Diabetes Technology & Therapeutics*, vol. 12, no. 3, pp. 173–177, 2010.

[39] R. Ziegler, G. Freckmann, and L. Heinemann, "Boluses in Insulin Therapy: A Commentary." *Journal of Diabetes Science and Technology*, pp. 1–7, Jun. 2016, ahead-of-print, doi:10.1177/1932296816653143.

[40] D. Luenberger, "Observers for multivariable systems," *IEEE Transactions on Automatic Control*, vol. 11, pp. 190–197, 1966.

[41] L. Kovács, B. Paláncz, and B. Zoltán, "Design of Luenberger Observer for Glucose-Insulin Control via *Mathematica*," *Proceedings of the 29th Annual International Conference of the IEEE EMBS*, pp. 624–627, 2007.

[42] C. Eberle and C. Ament, "The unscented Kalman Filter estimates the plasma insulin from glucose measurement," *BioSystems*, vol. 103, pp. 67–72, 2011.

[43] ——, "Real-time state estimation and long-term model adaptation: a two-sided approach toward personalized diagnosis of glucose and insulin levels," *Journal of Diabetes Science and Technology*, vol. 6(5), pp. 1148–58, 2012.

[44] P. Biswas, S. Bhaumik, and I. Patiyat, "Estimation of Glucose and Insulin Concentration using Nonlinear Gaussian Filters," *IEEE First International Conference on Control, Measurement and Instrumentation*, pp. 16–20, 2016.

[45] P. Palumbo, P. Pepe, S. Panunzi, and A. De Gaetano, "Observer-based glucose control via subcutaneous insulin administration," *8th IFAC Symposium on Biological and Medical Systems*, pp. 107–112, 2012.

[46] ——, "Time-Delay Model-Based Control of the Glucose-Insulin System, by means of a State Observer," *European Journal of Control*, vol. 6, pp. 591–606, 2012.

[47] ——, "Recent Results on Glucose-Insulin Predictions by means of a State Observer for Time Delay Systems," in *Prediction Methods for Blood Glucose Concentration*. Springer International Publishing, 2015, pp. 227–241.

[48] F. J. Doyle III, L. M. Huyett, J. B. Lee, H. C. Zisser, and E. Dassau, "Closed-Loop Artificial

Pancreas Systems: Engineering the Algorithms," *Diabetes Care*, vol. 37, pp. 1191–1197, 2014.

[49] S. Trevitt, S. Simpson, and A. Wood, "Artificial Pancreas Device Systems for the Closed-Loop Control of Type 1 Diabetes: What Systems Are in Development?" *Journal of Diabetes Science and Technology*, vol. 10, no. 3, pp. 714–723, 2016.

[50] C. Ellingsen, E. Dassau, H. Zisser, B. Grosman, M. W. Percival, L. Jovanovič, and F. J. Doyle III, "Safety Constraints in an Artificial Pancreatic β Cell: An Implementation of Model Predictive Control with Insulin on Board," *Journal of Diabetes Science and Technology*, vol. 3, no. 2, pp. 536–544, 2009.

[51] H. Zisser, L. Robinson, W. Bevier, E. Dassau, C. Ellingsen, F. Doyle III, and L. Jovanovic, "Bolus Calculator: A Review of Four "Smart" Insulin Pumps," *Diabetes Technology & Therapeutics*, vol. 10, no. 6, pp. 441–444, 2008.

[52] C. Toffanin, H. Zisser, F. J. Doyle III, and E. Dassau, "Dynamic insulin on board: incorporation of circadian insulin sensitivity variation." *Journal of Diabetes Science and Technology*, vol. 7, no. 4, pp. 928–940, 2013.

[53] F. H. El-Khatib, S. Russell, D. Nathan, R. G. Sutherlin, and E. R. Damiano, "A Bihormonal Closed-Loop Artificial Pancreas for Type 1 Diabetes," *Science Translational Medicine*, vol. 2, no. 27, p. 27ra27, 2010.

[54] H. Thabit, M. Tauschmann, J. M. Allen, L. Leelarathna, S. Hartnell, M. E. Wilinska, C. L. Acerini, S. Dellweg, C. Benesch, L. Heinemann, J. K. Mader, M. Holzer, H. Kojzar, J. Exall, J. Yong, J. Pichierri, K. D. Barnard, C. Kollman, P. Cheng, P. C. Hindmarsh, F. M. Campbell, S. Arnolds, T. R. Pieber, M. L. Evans, D. B. Dunger, R. Hovorka, APCam Consortium, and AP@home Consortium, "Home Use of an Artificial Beta Cell in Type 1 Diabetes." *The New England Journal of Medicine*, Sep. 2015.

[55] G. M. Steil, C. C. Palerm, N. Kurtz, G. Voskanyan, A. Roy, S. Paz, and F. R. Kandeel, "The Effect of Insulin Feedback on Closed Loop Glucose Control," *Endocrine Research*, vol. 96, pp. 1402–1408, 2011.

[56] A. Revert, F. Garelli, J. Picó, H. De Battista, P. Rossetti, J. Vehí, and J. Bondia, "Safety Auxiliary Feedback Element for the Artificial Pancreas in Type 1 Diabetes," *IEEE Transactions on Biomedical Engineering*, vol. 60, no. 8, pp. 2113–2122, 2013.

[57] J. L. Ruiz, J. L. Sherr, E. Cengiz, L. Carria, A. Roy, G. Voskanyan, W. V. Tamborlane, and S. A. Weinzimer, "Effect of Insulin Feedback on Closed Loop Glucose Control: A Crossover Study," *Journal of Diabetes Science and Technology*, vol. 6, pp. 1123–130, 2012.

[58] L. M. Huyett, E. Dassau, H. C. Zisser, and F. J. Doyle III, "Design and Evaluation of a Robust PID Controller for a Fully Implantable Artificial Pancreas," *Industrial and Engineering Chemistry Research*, vol. 54, pp. 10 311–10 321, 2015.

[59] B. W. Bequette, "Glucose clamp algorithms and insulin time-action profiles." *Journal of*

Diabetes Science and Technology, vol. 3, no. 5, pp. 1005–1013, 2009.

[60] R. Mantz, H. De Battista, and F. Bianchis, "Sliding mode conditioning for constrained processes," *Ind. Eng. Chem. Res*, vol. 43, no. 26, pp. 8251–8256, 2004.

[61] L. Magni, D. Raimondo, L. Bossi, C. Dalla Man, G. D. Nicolao, B. Kovatchev, and C. Cobelli, "Model Predictive Control of Type 1 Diabetes: An in Silico Trial," *Journal of Diabetes Science and Technology*, vol. 1, no. 6, pp. 804–812, 2007.

[62] P. Rossetti, C. Quirós, V. Moscardó, A. Comas, M. Giménez, F. J. Ampudia-Blasco, F. León, E. Montaser, I. Conget, J. Bondia, and J. Vehí, "Better Postprandial Glucose Control with a New Closed-Loop System as Compared with Open-Loop Treatment in Patients with Type 1 Diabetes," 76th Scientific Sessions American Diabetes Association, New Orleans, USA, Jul. 2016. [Online]. Available: http://www.abstractsonline.com/pp8/#!/4008/presentation/39723

[63] F. León-Vargas, F. Garelli, H. De Battista, and J. Vehí, "Postprandial response improvement via safety layer in closed-loop blood glucose controllers," *Biomedical Signal Processing and Control*, vol. 16, pp. 80–87, 2015.

[64] L.-X. Wang, *A Course in Fuzzy Systems and Control*. New Jersey, USA: Ed. Prentice-Hall, 1997.

[65] E. Atlas, R. Nimri, S. Miller, E. A. Grunberg, and M. Phillip, "MD-Logic Artificial Pancreas System: A Pilot Study in Adults with Type 1 Diabetes Mellitus," *Diabetes care*, vol. 33, no. 5, pp. 1072–1076, 2010.

[66] R. Mauseth, I. B. Hirsch, J. Bollyky, R. Kircher, D. Matheson, S. Sanda, and C. Greenbaum, "Use of a "fuzzy logic" controller in a closed-loop artificial pancreas." *Diabetes Technology & Therapeutics*, vol. 15, no. 8, pp. 628–633, Jul. 2013.

[67] R. Mauseth, S. M. Lord, I. B. Hirsch, R. C. Kircher, D. M. Matheson, and C. J. Greenbaum, "Stress testing of an artificial pancreas system with pizza and exercise leads to improvements in the system's fuzzy logic controller," *Journal of diabetes Science and Technology*, vol. 9, no. 6, pp. 1253–1259, 2015.

[68] R. Kircher, J. Lee, D. Matheson, and R. Mauseth, "Efficacy and Computational Efficiency of the Dose Safety Hypoglycemia Prevention Module (HPM)," *Diabetes Technology & Therapeutics*, vol. 17, pp. A97–A97, 2015.

[69] M. C. Riddell, D. P. Zaharieva, L. Yavelberg, A. Cinar, and V. K. Jamnik, "Exercise and the Development of the Artificial Pancreas: One of the More Difficult Series of Hurdles," *Journal of Diabetes Science and Technology*, vol. 9, no. 6, pp. 1217–1226, 2015.

[70] S. A. McAuley, J. C. Horsburgh, G. M. Ward, A. La Gerche, J. L. Gooley, A. J. Jenkins, R. J. MacIsaac, and D. N. O'Neal, "Insulin pump basal adjustment for exercise in type 1 diabetes: a randomised crossover study," *Diabetologia*, vol. 59, no. 8, pp. 1636–1644, 2016.

[71] N. Taleb, A. Emami, C. Suppere, V. Messier, L. Legault, J.-L. Chiasson, R. Rabasa-Lhoret,

and A. Haidar, "Comparison of Two Continuous Glucose Monitoring Systems, Dexcom G4 Platinum and Medtronic Paradigm Veo Enlite System, at Rest and During Exercise," *Diabetes Technology & Therapeutics*, vol. 18, no. 9, pp. 1–7, 2016.

[72] K. J. Bell, C. E. Smart, G. M. Steil, J. C. Brand-Miller, B. King, and H. A. Wolpert, "Impact of Fat, Protein, and Glycemic Index on Postprandial Glucose Control in Type 1 Diabetes: Implications for Intensive Diabetes Management in the Continuous Glucose Monitoring Era." *Diabetes care*, vol. 38, no. 6, pp. 1008–1015, 2015.

[73] S. Laxminarayan, J. Reifman, S. S. Edwards, H. Wolpert, and G. M. Steil, "Bolus Estimation—Rethinking the Effect of Meal Fat Content," *Diabetes Technology & Therapeutics*, vol. 17, no. 11, pp. 1–7, 2015.

[74] K. J. Bell, E. Toschi, G. M. Steil, and H. A. Wolpert, "Optimized Mealtime Insulin Dosing for Fat and Protein in Type 1 Diabetes: Application of a Model-Based Approach to Derive Insulin Doses for Open-Loop Diabetes Management," *Diabetes care*, pp. 1–4, Jul. 2016.

[75] H. A. Wolpert, A. Atakov-Castillo, S. A. Smith, and G. M. Steil, "Dietary fat acutely increases glucose concentrations and insulin requirements in patients with type 1 diabetes: implications for carbohydrate-based bolus dose calculation and intensive diabetes management." *Diabetes care*, vol. 36, no. 4, pp. 810–816, 2013.

[76] L. A. Gonder-Frederick, J. H. Grabman, B. Kovatchev, S. A. Brown, S. Patek, A. Basu, J. E. Pinsker, Y. C. Kudva, C. A. Wakeman, E. Dassau, C. Cobelli, H. C. Zisser, and F. J. Doyle, "Is Psychological Stress a Factor for Incorporation Into Future Closed-Loop Systems?" *Journal of Diabetes Science and Technology*, 2016.

TABLE 1. Low and intermediate complexity models widely used in the artificial pancreas field.

	Bergman model [22]	Hovorka model [23]	Identifiable Virtual Patient model [28]
Carb. absorp.	N/A	$U_G(t) = \frac{D_G A_G t e^{-t/t_{maxG}}}{t_{maxG}^2}$	$R_A(t) = \frac{D_G A_G t e^{-t/t_{maxG}}}{V_G t_{maxG}^2}$
S.c. insulin PK	N/A	$\dot{S}_1(t) = u_{SC}(t) - \frac{S_1(t)}{t_{maxI}}$ $\dot{S}_2(t) = \frac{S_1(t)}{t_{maxI}} - \frac{S_2(t)}{t_{maxI}}$ $\dot{I}(t) = \frac{S_2(t)}{t_{maxI} V_I} - k_e I(t)$	$\dot{I}_{SC}(t) = -\frac{I_{SC}(t)}{\tau_1} + \frac{u_{SC}(t)}{\tau_1 K_{cl}}$ $\dot{I}(t) = -\frac{I(t)}{\tau_2} + \frac{I_{SC}(t)}{\tau_2}$
Insulin action	$\dot{X}(t) = -p_2 X(t) + p_3(I(t) - I_b)$	$\dot{X}_1(t) = -k_{a1} X_1(t) + k_{b1} I(t)$ $\dot{X}_2(t) = -k_{a2} X_2(t) + k_{b2} I(t)$ $\dot{X}_3(t) = -k_{a3} X_3(t) + k_{b3} I(t)$	$\dot{I}_E(t) = -p_2 I_E(t) + p_2 S_I I(t)$
Glucose metab.	$\dot{G}(t) = -(p_1 + X(t))G(t) + p_1 G_b + \frac{U_G(t)}{V_G}$	$\dot{Q}_1(t) = -X_1 Q_1(t) + k_{12} Q_2(t) - F_{01}^c(t) - F_R(t) + U_G(t) + EGP_0(1 - X_3(t))$ $\dot{Q}_2(t) = X_1 Q_1(t) - k_{12} Q_2(t) - X_2(t) Q_2(t)$ $G(t) = \frac{Q_1(t)}{V_G}$	$\dot{G}(t) = -(GEZI + I_E(t))G(t) + EGP + R_A(t)$

TABLE 2. Summary of publications addressing the design of observers in the context of diabetes.

Reference	Model	Observer	Validation	Evaluation
Wilinska *et al.*, 2012 [31]	Hovorka	Kalman	N/A	N/A
Gondhalekar *et al.*, 2013 [32]	Linear	Luenberger	N/A	N/A
Lee *et al.*, 2014 [34]	Linear	Luenberger, MHSE	Simulation	SSE
Pereda *et al.*, 2015 [35]	Hovorka	EKF	Simulation & data from DM1 subjects	RMSE and MARD
Boiroux *et al.*, 2015 [37]	MVP	UKF	Simulation	Median time in hyperglycemia, within target or hypoglycemia
Kovács *et al.*, 2007 [41]	Bergman	Luenberger	Simulation	Graphs
Eberle and Ament, 2011 [42]	Bergman	EKF, UKF, PF	Simulation	RMSE
Eberle and Ament, 2012 [43]	Bergman	UKF	Simulation & data from pigs	Graphs
Biswas *et al.*, 2016 [44]	Bergman	UKF, CQKF, GHF	Simulation	RMSE
Palumbo *et al.*, 2012-15 [45], [46], [47]	DDE	Nonlinear	Simulation	Amount of hypoglycemic events and plasma glycemia

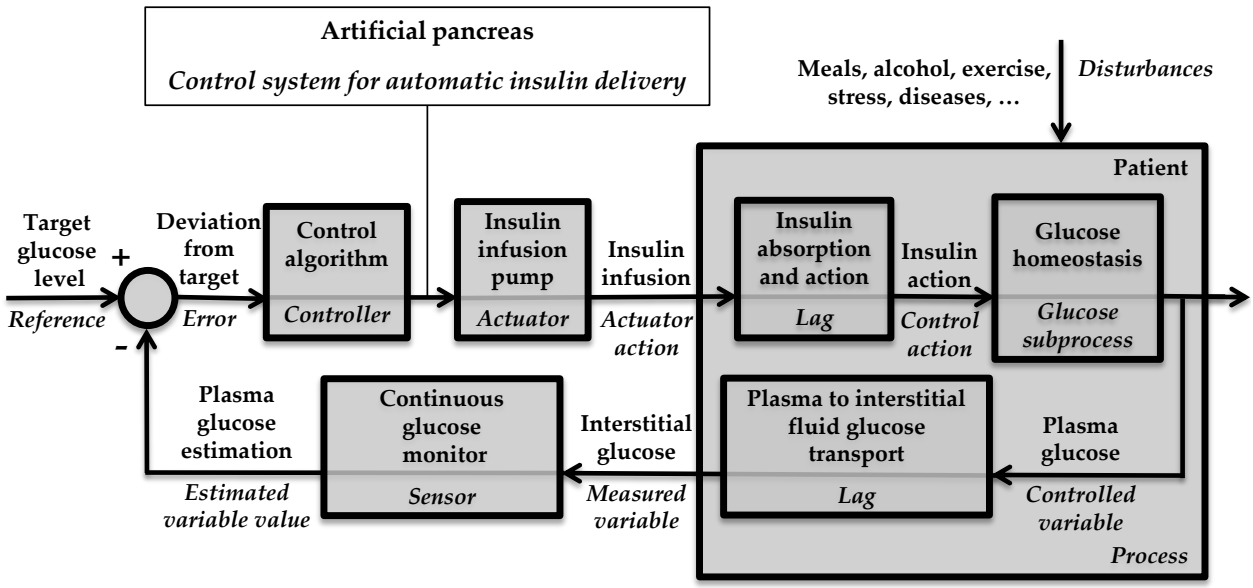

Figure 1. The artificial pancreas as a classic closed-loop glucose control system (medical vocabulary in bold and control engineering vocabulary in italics).

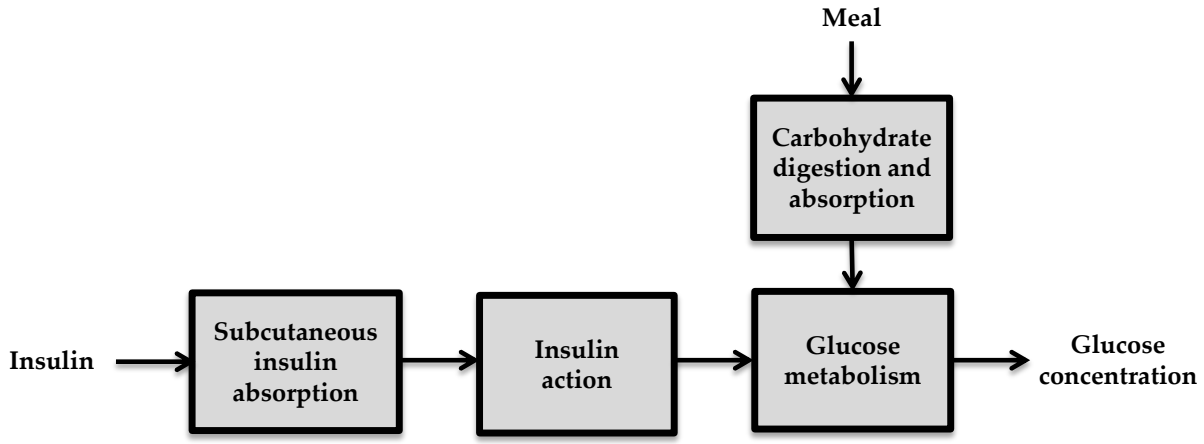

Figure 2. Model components for the glucose-insulin system.

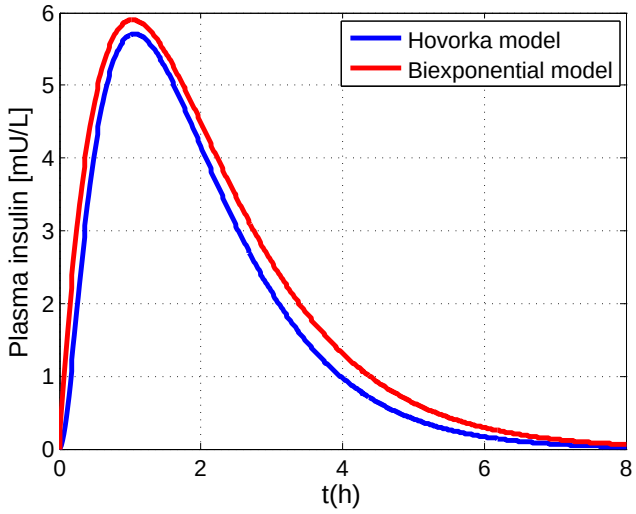

Figure 3. Comparison of the unit impulse response of Hovorka insulin pharmacokinetic model [23] and the biexponential model [30] with nominal parameters (Hovorka: $t_{maxI} = 55$ min, $k_e = 0.138$ min^{-1}, $V_I = 0.12$ L/Kg, body weight 70 Kg; biexponential: $\tau_1 = 55$ min, $\tau_2 = 70$ min, $K_{cl} = 1$ L/min).

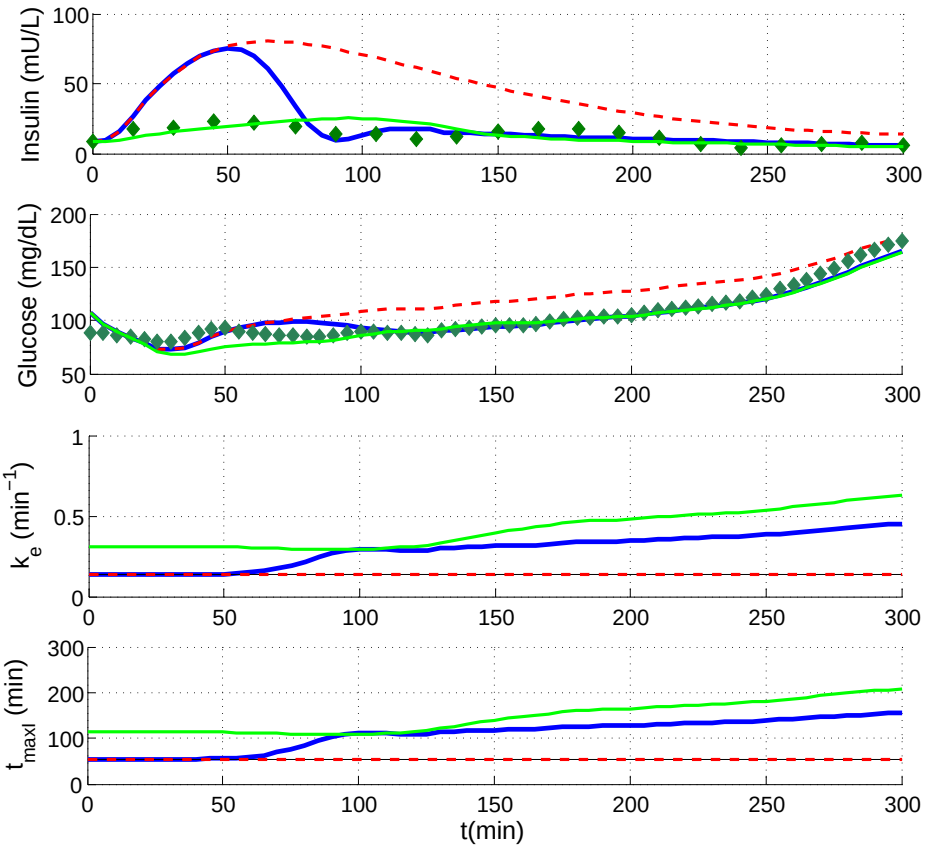

Figure 4. Example of performance of the insulin observer in [35] for a sample patient. Dashed red line represents the case with nominal pharmacokinetic parameters in the Hovorka model; solid blue line the case with real-time adaptation of k_e and t_{maxI} with initial values set to nominal values; and solid green line the case with real-time adaptation of k_e and t_{maxI} with initial values set to the average of the parameter values estimated for the rest of patients. Green diamonds represent measurements (adapted from [35]).

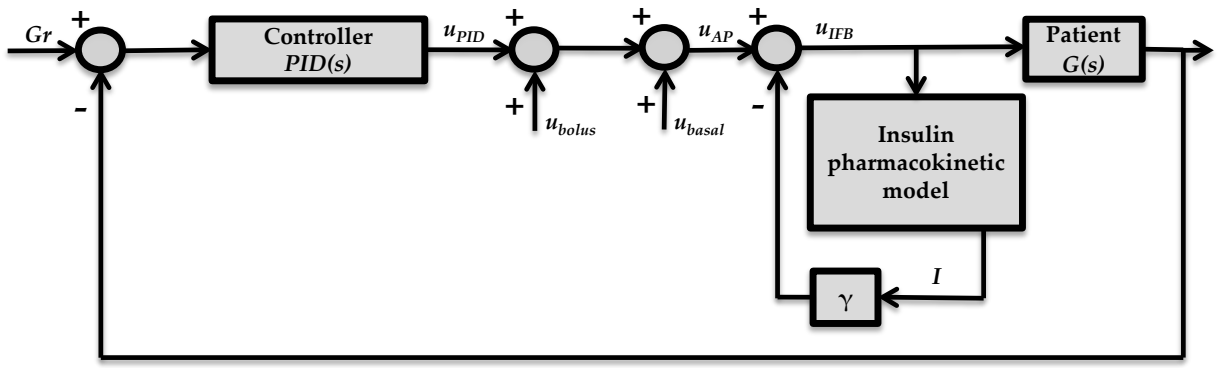

Figure 5. Block diagram for an artificial pancreas controller with Insulin Feedback (IFB).

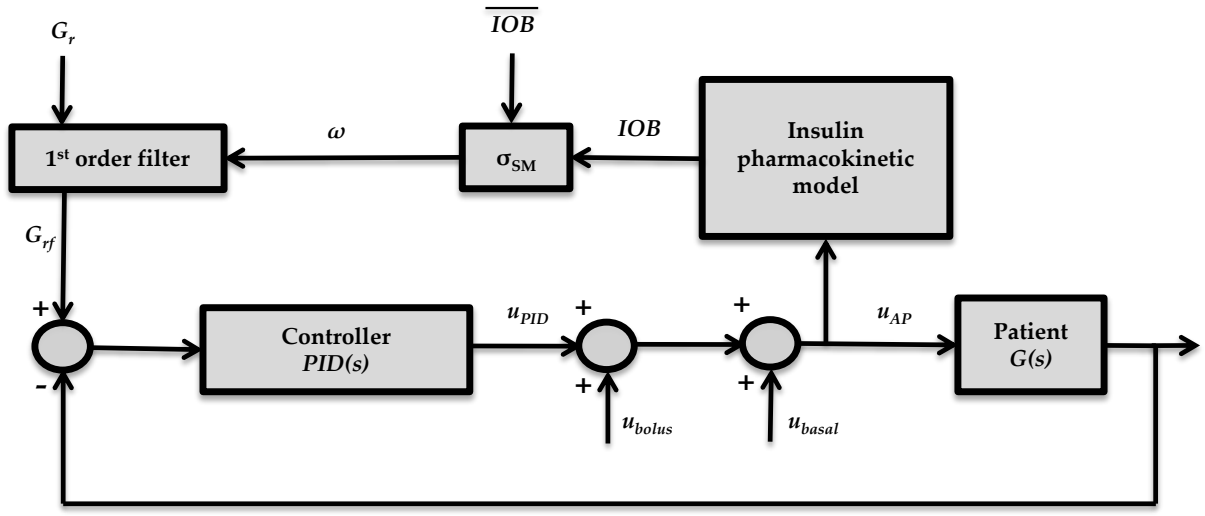

Figure 6. Block diagram for an artificial pancreas controller including the Sliding Mode Reference Conditioning (SMRC) control structure.

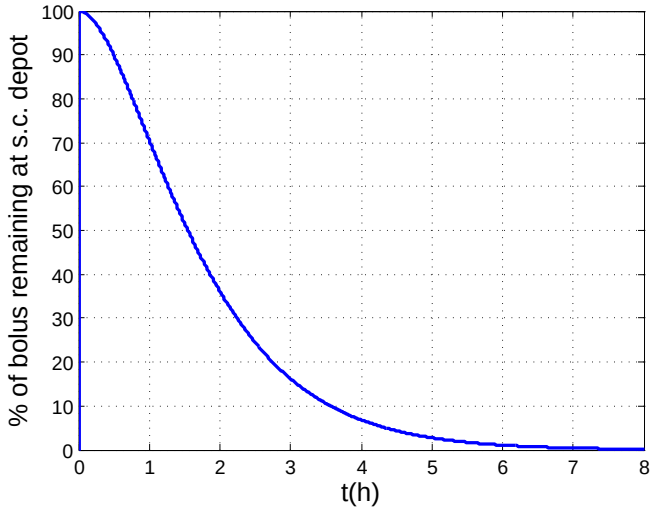

Figure 7. Time profile of subcutaneous insulin depot as a percentage of the bolus size administered at t=0 according to the model (26)-(28) ($t_{maxI} = 55$ min).

Sidebar: Models and variability

The large intra-subject variability in the patient's response represents a big challenge for modeling, since it may jeopardize any identification process giving rise to individualized patient models representing only an "average" behavior with limited prediction accuracy. From the mathematical perspective, variability entails uncertainty in model parameters and initial conditions. Simulation tools for models with uncertainty can thus be helpful to understand the impact of intra-subject variability in the accuracy of model predictions, as well as implementing more robust algorithms for the artificial pancreas.

A natural way to describe uncertainty in model parameters and initial conditions is through the representation of values as intervals, giving rise to "interval models" [S1]. The output of an interval model is an envelope enclosing all possible glucose trajectories (for each possible value in the interval), instead of a single trajectory as it is the case with a standard set of differential equations. Envelopes should be efficiently computed with mathematical guarantee, that is, they must include all possible responses with the minimum possible overestimation. Interval methods [S2] generally lead to divergent envelopes and Monte Carlo simulation [S3] is not applicable since the inclusion condition is not guaranteed. Other tools as the differential inclusions can be efficient under certain cooperative conditions (see [S4]), but unfortunately, they are not useful for glucose-insulin models. Nowadays, new techniques as differential inequalities and monotone dynamical systems (see [S5], [S6] and the references therein) have been implemented. In fact, monotone systems theory has been successfully used for the prediction of an envelope containing all the possible glycemic responses since, in some cases, it is possible to calculate the exact envelope for all possible behaviors [S7].

The interconnection of monotone systems may be studied by considering a flow $\mathbf{x}(t) = \phi(\mathbf{x_0}, t)$. A system is monotone if

$$\mathbf{x_0} \preceq \mathbf{y_0} \Rightarrow \phi(\mathbf{x_0}, t) \preceq \phi(\mathbf{y_0}, t), \tag{S1}$$

for all $t \geq 0$, where $\preceq$ is a given relation order [S4], as represented in Figure S1.

From analytical point of view (see [S4]), the rate of change of the state vector $\mathbf{x} = (x_1, \ldots, x_n)^T$ of a monotone system can be described as

$$\frac{d\mathbf{x}}{dt} = \mathbf{f}(\mathbf{x}, \mathbf{p}, \mathbf{u}(t)), \tag{S2}$$

where the vector function $\mathbf{f} = (f_1, \ldots, f_n)^T$ satisfies the following property:

$$\frac{\partial f_i}{\partial x_j} \cdot \frac{\partial f_j}{\partial x_i} \geq 0, \quad \text{for all } i \neq j,\ t \in \mathbb{R}^+. \tag{S3}$$

In particular, for cooperative systems [S7], the relation order is induced by the corresponding positive orthant, which is characterized by a Metzler Jacobian Matrix, that is,

$$\frac{\partial f_i}{\partial x_j} \geq 0, \quad \text{for all } i \neq j,\ t \geq 0. \tag{S4}$$

Monotonicity can be also characterized by using a species graph, in which a node is assigned to each state, parameter, input and output, and a *spin assignment* is carried out for each node based on the sign of partial derivatives (see [S5]). Moreover, the monotonicity of the system with respect to the parameters of the model can be analyzed by considering the parameters as system states in an extended model [S8].

In [S9] tight glucose envelopes were obtained for models of certain complexity like Hovorka model [23], under uncertain input, initial state and model parameters with little computational complexity. For an illustration, Figure S2 shows the envelopes for plasma glucose and plasma insulin concentrations, for the interval Hovorka simulator developed in [S9], considering an uncertainty of $\pm 30\%$ in time-to-peak plasma insulin concentration, t_{maxI} , while the rest of the model parameters are kept at their nominal value. A prediction horizon of 150 min is considered. Reported variability of this single pharmacokinetic parameter yields to a glucose concentration after 150 min ranging from 84 mg/dL to 154 mg/dL, that is, almost a twofold difference. Variability in insulin sensitivity and meal intake would increase further this range, as well as uncertainty in initial conditions of the model state. A maximum envelope width of approximately 12 mU/L is produced for plasma insulin concentration, which corresponds to more than twice its basal value.

To conclude, interval models embed variability into the patient's model [S10] and can be useful in worst-case approaches for an increased robustness. In any case, robustness to prediction errors and model adaptation are essential features of an artificial pancreas.

References

[S1] J. Bondia and J. Vehí, "Physiology-Based Interval Models: A Framework for Glucose Prediction Under Intra-patient Variability," in *Prediction Methods for Blood Glucose Concentration*. Springer International Publishing, 2015, pp. 159–181.

[S2] N. S. Nedialkov and K. R. Jackson, "An interval Hermite-Obreschkoff method for computing rigorous bounds on the solution of an initial value problem for an ordinary differential equation," *Reliable Computing*, vol. 5, no. 3, pp. 289–310, 1999.

[S3] R. Calm, M. García-Jaramillo, J. Bondia, M. Sainz, and J. Vehí, "Comparison of interval and Monte Carlo simulation for the prediction of postprandial glucose under uncertainty

in type 1 diabetes mellitus," *Computer Methods and Programs in Biomedicine,*, vol. 104, no. 3, pp. 325–332, 2011.

[S4] M. Kieffer and E. Walter, "Guaranteed nonlinear state estimator for cooperative systems," *Numerical Algorithms*, vol. 37, no. 1, pp. 187–198, 2004.

[S5] E. Sontag, "Monotone and near-monotone biochemical networks," *Systems and Synthetic Biology*, vol. 1, no. 2, pp. 59–87, 2007.

[S6] K. Bondar, "Some scalar difference inequalities," *Applied Mathematical Sciences*, vol. 5, no. 60, pp. 2951–2956, 2011.

[S7] H. Smith, *Monotone dynamical systems: An introduction to the theory of competitive and cooperative systems*. AMS Bookstore, 2008.

[S8] V. Puig, A. Stancu, and J. Quevedo, "Simulation of uncertain dynamic systems described by interval models: A survey," in *16th IFAC World Congress*, 2005.

[S9] D. de Pereda, S. Romero-Vivó, B. Ricarte, and J. Bondia, "On the prediction of glucose concentration under intra-patient variability in type 1 diabetes: A monotone systems approach," *Computer Methods and Programs in Biomedicine*, vol. 108, no. 3, pp. 993–1001, 2012.

[S10] A. J. Laguna, P. Rossetti, F. J. Ampudia-Blasco, J. Vehí, and J. Bondia, "Experimental blood glucose interval identification of patients with type 1 diabetes," *Journal of Process Control*, vol. 24, no. 1, pp. 171–181, 2014.

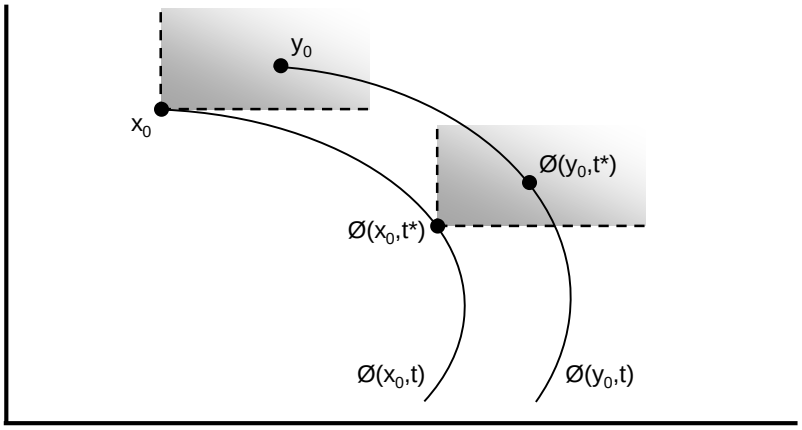

Figure S1. Relation order in the flow of a monotone system.

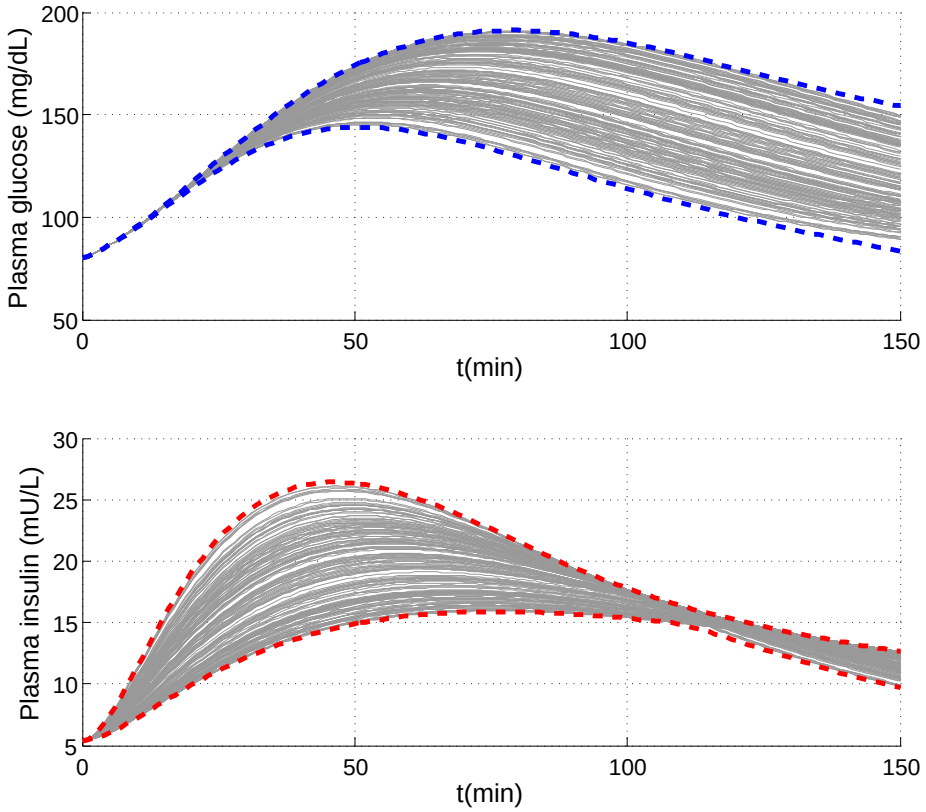

Figure S2. Plasma glucose (top) and plasma insulin (bottom) concentration envelopes of Hovorka model for an uncertainty of $\pm 30\%$ in parameter t_{maxI}, as computed by the simulator in [S9]. Monte Carlo simulations are also presented in grey color for comparison.

Sidebar: Observability of nonlinear systems

The property of observability measures how well internal states of a system can be deduced by knowledge of its external outputs. A dynamical system is called observable on a finite time interval $[t_0, t_f]$ if any initial state $x(t_0) = x_0$ is uniquely determined by the corresponding output $y(t)$ for $t \in [t_0, t_f]$.

All physiological glucose-insulin models belong to the category of nonlinear models. The observability of a nonlinear system

$$\dot{x}(t) = f(x(t), u(t)), \tag{S5}$$

$$y(t) = h(x(t)), \tag{S6}$$

can be analyzed by means of analytical methods, through the Lie derivatives [S11], or by numerical methods, through the empirical observability Gramian [S12]. Both of them have been used in type 1 diabetes research. In particular, Lie derivatives are used in [35] (Hovorka model) and [42] (Bergman model), and the empirical observability Gramian in [43] (Bergman model).

Lie derivatives

The Lie derivative of $h(x)$ with respect to $f(x, u)$ is defined as $L_{f(x,u)}h(x) = \nabla h(x) f(x, u)$ and it is calculated recursively as follows:

$$L^i_{f(x,u)}h(x) = L_{f(x,u)}(L^{(i-1)}_{f(x,u)}h(x)), \qquad \text{if } i = 1, 2, ...$$
$$L^0_{f(x,u)}h(x) = h(x).$$

The system (S5)-(S6) is considered observable if the following Jacobian matrix

$$\frac{\partial}{\partial x}\begin{bmatrix} h(x) \\ L_{f(x,u)}h(x) \\ \cdots \\ L^{n-1}_{f(x,u)}h(x) \end{bmatrix} \tag{S7}$$

has rank n, where n is the system order.

Empirical observability Gramian

The Gramian observability matrix W_0 is also determined for observability analysis. This matrix quantifies generalized energy transfer E_0 from initial state x_0 to the output within an infinite time horizon:

$$E_0 = \int y^T(\tau) y(\tau) d\tau = x_0^T W_0 x_0. \tag{S8}$$

The Gramian observability matrix can be computed from experimental or simulation data within a region where the process is to be operated (see [43], [S12], [S13] for details). In these cases, it is called the empirical observability Gramian. For nonlinear systems, each state is normalized such that its energy transfer to the output is equal to one. Then, its singular values, must be determined. The smallest singular value, λ, quantifies the energy transfer from the least observable state to the outputs. A system is considered unobservable if $\lambda = 0$, and practically observable if $\lambda > 0.1$. Moreover, $\lambda < 0.1$ for the normalized system indicates that the signal-to-noise ratio might be too small for a reliable state estimation.

It is worth remarking that even when the system is observable, difficulties in the reliable estimation of pharmacokinetic parameters may arise due to non-identifiability issues. The "a priori" or structural identifiability property of a model indicates if the parameters of the model can be determined assuming that all observable variables are error-free. Lack of structural identifiability arises due to the model structure only and it is independent of the amount and quality of the given experimental data. However, a parameter that is structurally identifiable may still be practically non-identifiable. This can arise due to insufficient amount and quality of experimental data or the chosen measurement time points. Common problems in the identification of glucose-insulin models are the lack of excitability of basal insulin, which is rarely variable enough, especially during the night, and the administration of insulin boluses at mealtime, making difficult to separate the meal and insulin effects on glucose after meal intake.

References

[S11] R. Hermann and A. J. Krener, "Nonlinear controllability and observability," *IEEE Transactions on Automatic Control*, vol. 22, pp. 728–740, 1977.

[S12] D. Geffen, D. Findeisen, M. Schliemann, F. Allgower, and M. Guay, "Observability based parameter identifiability for biochemical reaction networks," *American Control Conference*, 2008.

[S13] S. Lall, J. Marsden, and S. Glavaski, "A subspace approach to balanced truncation for model reduction of nonlinear control systems," *International Journal of Robust and Nonlinear Control*, vol. 12, pp. 519–535, 2002.

Sidebar: Kalman filter extensions to nonlinear systems

Physiological variability can be represented as noise in the system dynamics. Besides, the use of sensors also introduce noise into the measurements. If stochastic properties of these noise sources are available, state estimation may be performed more effectively than simply using sensor signals as noise-free signals and estimating the state based on noise-free state transition model. Rudolph Kalman investigated this problem and developed the widely used **Kalman filter** [S14]. Originally, he addressed the general problem of estimating the state $x \in \mathbb{R}^n$ of a discrete-time controlled process that is governed by the linear stochastic difference equations

$$x(k+1) = Ax(k) + Bu(k) + w(k), \quad w(k) \sim N(0, Q), \tag{S9}$$

$$y(k) = Cx(k) + v(k), \quad v(k) \sim N(0, R), \tag{S10}$$

where $y \in \mathbb{R}^r$ are the measurements and the random variables $w(k)$ and $v(k)$ represent the process and measurement noise, which are assumed to be independent, white and with normal probability distributions of variances Q and R, respectively. The Kalman filter provides an efficient computational method to estimate the state of a process in a way that minimizes the mean of the squared error in a two-step process: the prediction step (the current state estimate is projected ahead in time) and the correction step (the projected estimate is adjusted by an actual measurement).

Since the time of its introduction, the Kalman filter has been the subject of extensive research and application. The Kalman filter theory has been extended to nonlinear processes, given by

$$x(k) = f(x(k-1), u(k-1)) + w(k-1), \quad w(k-1) \sim N(0, Q), \tag{S11}$$

$$y(k) = h(x(k)) + v(k), \quad v(k) \sim N(0, R), \tag{S12}$$

where $f(x(k-1), u(k-1))$ defines the system dynamics and $h(x(k))$ denotes the measurement function. For that, this kind of systems are transformed through a linearization procedure known as **Extended Kalman Filter** (EKF) [S15], [S16], or by an unscented transformation called **Unscented Kalman Filter** (UKF) [S17], [S18], [S19]. The use of the EKF has two well-known drawbacks in practice: linearization can produce highly unstable filters if the assumption of local linearity is violated. Besides, the derivation of the Jacobian matrices are nontrivial in most applications and often lead to significant implementation difficulties. These disadvantages may be overcome with the use of the UKF. It is based on the Unscented Transformation (UT), which is a deterministic sampling approach to capture mean and covariance estimates with a minimal set of $2n + 1$ state sample points, called sigma points, based on a square-root decomposition of the prior covariance. These sigma points are propagated through the nonlinearity, without

approximation, and a weighted mean and covariance is found. The sigma points are chosen so that their sample mean and sample covariance are in agreement with the mean $\bar{x}$ and covariance P of the n-dimensional random variable x. The underlying idea is to approximate the probability distribution instead of the function (see Figure S3).

Moreover, Kalman filter extensions can also be used in continuous-time systems that are represented by differential equations

$$\dot{x}(t) = f(x(t), u(t)) + w(t), \quad w(t) \sim N(0, Q(t)), \tag{S13}$$

$$y(t) = h(x(t)) + v(t), \quad v(t) \sim N(0, R(t)), \tag{S14}$$

after a discretization procedure. The glucose-insulin models found in the literature belong to this kind of systems.

References

[S14] R. Kalman, "A New Approach to Linear Filtering and Prediction Problems," *Transaction of the ASME Journal of Basic Engineering*, vol. 82(Series D), pp. 35–45, 1960.

[S15] P. Maybeck, "Stochastic models, estimation, and control," *Math Sci Eng*, vol. 141, p. 423 pp, 1979.

[S16] G. Smith, S. Schmidt, and L. McGee, "Application of statistical filter theory to the optimal estimation of position and velocity on board a circumlunar vehicle," *Technical Report of the National Aeronautics and Space Administration*, vol. NASA TR R-135, 1962.

[S17] S. Julier and J. K. Uhlmann, "New extension of the Kalman filter to nonlinear systems," *AeroSense'97*, pp. 182–193, 1997.

[S18] ——, "Unscented filtering and nonlinear estimation," *Proceedings of the IEEE*, vol. 92(3), pp. 401–422, 2004.

[S19] E. Wan and R. van der Merwe, "The unscented Kalman Filter for nonlinear estimation," *Proceeding of the IEEE Symposium AS-SPCC*, pp. 153–158, 2000.

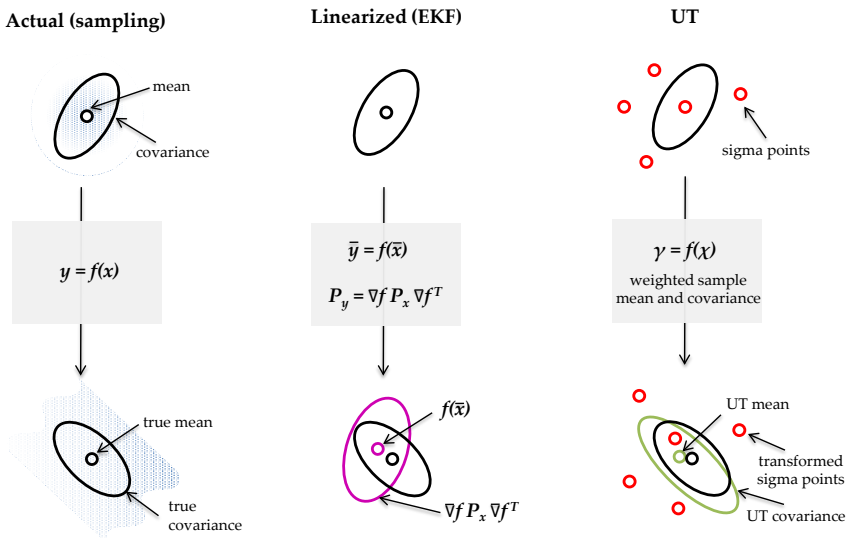

Figure S3. Example of the Unscented Transformation (UT) for mean and covariance propagation, compared to the Extended Kalman Filter (EKF) (adapted from [S19]).

Sidebar: Why is insulin estimation and prediction needed in an artificial pancreas?

In order to keep glucose levels of patients affected by type 1 diabetes in a safe range, the artificial pancreas can be used as a closed-loop control system that automatically dispenses insulin. However, the use of insulin as control action has different limitations:

- Insulin has a unidirectional effect lowering glucose values. Any insulin excess cannot be compensated beyond pump switch-off, and external actions are required like meal consumption or glucagon administration.
- Insulin is delivered subcutaneously, as opposed to the pancreas which delivers insulin into blood. The lag introduced by subcutaneous insulin absorption amounts to 50 minutes. Control action peak is reached after another 30 minutes, with a total dynamic lag of 80 minutes. An excessive insulin infusion might thus provoke hypoglycemia later. Severe hypoglycemia can lead to comma and death.

Therefore, mechanisms are necessary to avoid an excess of insulin within the patient's body. They rely upon the prediction of plasma insulin or insulin-on-board, the injected insulin that didn't have an effect yet, from subcutaneous insulin pharmacokinetic models. Control action is then modulated accordingly. However, high variability of insulin pharmacokinetics suggests that real-time estimation of pharmacokinetic parameters and signals is also needed for a better and safer performance. This can be addressed with the design of insulin observers.

Author Biography

Dr. Jorge Bondia received an M.Sc. degree in Computer Science in 1994, and the Ph.D. degree in Control Engineering in 2002 both from the Universitat Politècnica de València, Spain. He is Associate Professor since 2007 and holds the accreditation to Full Professor since 2015. He has been teaching since 1995 at the Systems Engineering and Control Department, Universitat Politècnica de València, on subjects in the fields of automation, control engineering and biomedical engineering. He develops his research activity as a member of the University Institute of Control Systems and Industrial Computing (Institute ai2), where he started a research line on diabetes technology and the artificial pancreas in 2004. His main research lines are modeling of type 1 diabetes pathophysiology, intra-patient variability and glucose prediction under uncertainty, tools for insulin therapy optimization, new calibration algorithms for accuracy improvement of continuous glucose monitoring and control algorithms for an efficient and safe artificial pancreas. He has published more than 40 articles on the artificial pancreas and contributed to more than 100 conferences. He is currently the Head of the MEDERI Living Lab at Institute ai2, dedicated to new technologies for chronic diseases, rehabilitation and health education. Corresponding author: jbondia@isa.upv.es. Dep. Ing. de Sistemas y Automtica, Universitat Politècnica de València, C/ Camino de Vera, s/n, 46022 Valencia, Spain

Dr. Sergio Romero-Vivó received an M.Sc. degree in Mathematics in 1996 from the Universidad de Valencia, Spain. Currently, he is Associate Professor at the Universidad Politècnica de València where he obtained the Ph.D. degree in 2001 with a thesis on "Controllability and Reachability of Positive Linear Control Systems". He is an active member of the University Institute of Multidisciplinary Mathematics and his research interests specialize on matrix analysis, structural properties of multi-dimensional positive systems, and uncertainty dynamical systems and their applications to biomedical control models.

Dr. Beatriz Ricarte received an M.Sc. degree in Agricultural Engineering in 1997, and the Ph.D. in Mathematics in 2003 both from Universitat Politècnica de València, Spain. She has been teaching at the same university since 2001 at the Department of Applied Mathematics where she is currently Associate Professor. She develops her research activity as a member of the University Institute of Multidisciplinary Mathematics in topics of matrix analysis and its application to mathematical modeling of biological systems and control theory. She is member of the International Linear Algebra Society (ILAS) and the Spanish Society of Applied Mathematics (SEMA). She is also a member of the Editorial Board of the Open Journal of Modeling and Simulation. She is currently holding the Secretary responsibility in the School of Agricultural Engineering and Environment from UPV. The Secretary is the public authenticator of School events and agreements, and assists the Head in organization and administration tasks.

Dr. José Luis Díez received an M.Sc. degree in Industrial Engineering in 1995, and the Ph.D. degree in Control Engineering in 2003 both from the Universitat Politècnica de València, Spain. He is currently an Associate Professor and he has been teaching since 1995 at the Systems Engineering and Control Department, Universitat Politècnica de València, in a wide range of subjects in the area such as automation, linear systems control theory, digital signal processing, and intelligent systems. His research interests include complex systems modeling and identification (biomedical, biological, energy and social systems), data mining, clustering techniques, intelligent control, and control education.